91-04723/

EFFECT OF BORON ON PRECIPITATION AND RECRYSTALLIZATION KINETICS IN HOT DEFORMATION OF TITANIUM-NIOBIUM MICROALLOYED STEELS

Final Report by

M. Djahazi, T.L. Mavropoulos, X.L. Hé and J.J. Jonas

McGill University
Montreal, Quebec
H3A 2A7

Work on this project was conducted under the auspices of the Canada Centre for Mineral and Energy Technology, Energy, Mines and Resources Canada

106 pp

MICROMEDIA

DSS File Number	:	12ST.23440-4-9057
DSS Contract Serial Number	:	OST84-00179
CANMET Project Number	:	
CANMET Scientific Authorigy	:	Dr. G.E. Ruddle

EXECUTIVE SUMMARY

Experiments have been carried out regarding the influence of boron addition on the recrystallization and precipitation behaviour of Nb steels. The results clearly indicate that B addition *on its own* retards recrystallization only slightly, whereas it has significant retarding effects when added in combination with Nb. This effect is equivalent to an increase in the pancaking temperature by 30 to 50°C. Similar, but reduced, interactions are expected between B and Ti, Mo or V.

The present observations reveal that the addition of B to Nb steels leads to an *increase* in the precipitation rate of the Nb carbides. This acceleration, which is largely responsible for the retardation of recrystallization described above, can be attributed to the attendant increase in the concentration of the interstitial elements, which increases in turn the driving force for precipitation. A further role is played by the temporary segregation of B to dislocations and grain boundaries.

The use of PTA (particle tracking autoradiography) has shown that, under industrial rolling conditions, the *temporary* segregation of B is considerably more important than the equilibrium variety. Such temporary segregation can be caused by cooling or by deformation. In both cases, an excess vacancy concentration is produced, which migrates to grain boundary (and dislocation) sinks. The vacancies link up with B atoms in the form of complexes; the B is deposited at the boundaries when the vacancies are annihiliated there. A further component of temporary segregation is caused by the sweeping action of the grain boundaries during recrystallization.

The temporary segregation of B to grain boundaries under rolling conditions is probably accompanied by the non-equilibrium segregation of other elements. Such phenomena appear to be fertile subjects for further investigation.

SOMMAIRE

Des expériences ont été effectuées pour étudier l'influence d'une addition de bore sur les processus de recristallisation et de précipitation des aciers au niobium. Les résultats indiquent clairement qu'une addition de B seul affecte peu la recristallisation, alors qu'en présence de Nb, il la retarde de façon significative. Cet effet est équivalent à une augmentation de 30 à 50°C de la température de non-recristallisation. De même, des interactions entre B et Ti, Mo ou V peuvent exister mais de façon moins importante.

Les résultats de l'étude indiquent que l'addition du B dans les aciers au Nb accroît la vitesse de précipitation des carbures de Nb. Cette accélération, qui est en grande partie responsable du retard à la recristallisation de l'austénite décrit ci-dessus, peut être attribué à une augmentation de la concentration des éléments interstitiels qui en fin de compte accroît la force motrice de la précipitation. La ségrégation temporaire du B sur les dislocations et aux joints de grain peut également jouer un rôle supplémentaire.

L'utilisation de la technique de l'alphagraphie (PTA) a montré que dans des conditions de laminage industrielles, la ségrégation temporaire est beaucoup plus importante que la ségrégation d'équilibre. Elle peut être produite par le refroidissement ou par la déformation. Dans les deux cas, un excès de concentration de lacunes est créé, lesquelles migrent aux joints de grain et sur les dislocations. Les lacunes interagissent avec les atomes de B pour former des complexes; le B est déposé aux joints lorsque les lacunes y sont annihilées. Une autre cause de la ségrégation temporaire est le mouvement de balayage des joints de grain durant la recristallisation.

La ségrégation temporaire du B aux joints de grain, sous des conditions de laminage, est probablement accompagnée par la ségrégation hors d'équilibre d'autres éléments. De tels phénomènes semblent être fructueux pour de futures études.

EFFECT OF BORON ON PRECIPITATION AND RECRYSTALLIZATION KINETICS IN HOT DEFORMATION OF TITANIUM-NIOBIUM MICROALLOYED STEELS

AIM:

According to the contract, the objectives of the present investigation were the following. To conduct experimental research to determine the effects of boron addition on the kinetics of austenite recrystallization and carbonitride precipitation in relation to the design of microalloying composition and thermomechanical processing (controlled rolling) of titanium-niobium steels for high strength and toughness applications.

ORGANIZATION OF THE WORK:

The research performed under this contract was divided into three parts, which can be described as follows:

(i) Effect of B Addition on Recrystallization Kinetics. This part of the investigation was carried out by T.L. Mavropoulos, who prepared a full account of his work in the Ph.D. thesis submitted in October, 1986. Dr. Mavropoulos is now employed at the Noranda Research Centre. He has written up the principal features of his results in the form of two research papers, which have been submitted to the

Canadian Metallurgical Quarterly. The contents of these reports, which are attached, will be summarized briefly below. For further details, the reader is referred to the Mavropoulos thesis, which has been made available to PMRL, CANMET.

(ii) Effect of B Addition on Precipitation Kinetics. The precipitation characteristics of the current steels were investigated by M. Djahazi, who is preparing a Ph.D. thesis on this subject at McGill. Although his part of the project is far from complete, his preliminary results have been described in two recent papers, which are also attached. The main features of his observations will be described below in summary form.

(iii) The Non-Equilibrium Segregation of Boron. Many of the metallurgical effects of boron addition can be attributed to its segregation at austenite grain boundaries. McGill has been fortunate to play host during the past year to Dr. Xin Lai Hé of the Beijing University of Iron and Steel Technology. He is the foremost international specialist on the non-equilibrium segregation of boron and has been carrying out research on this topic in our laboratory. He has prepared two detailed reports of his observations to date (including some of his work in China). These observations will also be summarized below, and his manuscripts are attached to this report for reference purposes (and because of the usefulness of some of his techniques and analyses).

PART I EFFECT OF B ADDITION ON THE RECRYSTALLIZATION OF AUSTENITE

Summary of the Method

Four low carbon bainitic steels were compression tested under interrupted and continuous loading conditions. These materials were made from a base steel containing 0.026% C, to which were added one or both of 0.055% Nb and/or 30 ppm of B. In this way, the influence on the rapidity of recrystallization of additions of (i) Nb; (ii) B; and (iii) Nb + B was assessed independently. The recrystallization kinetics of the hot worked austenite were determined for prestrains of 0.12, 0.25 and 0.50 in the temperature range 900 to 1100°C. The observations indicate that the addition of B is most effective in retarding recrystallization in the presence of Nb. Furthermore, the degree of retardation is influenced by both the prestrain and the temperature.

Carbon extraction replicas were prepared and particle tracking autoradiography was employed to provide experimental evidence regarding the state of solution of the B during deformation or cooling and subsequent holding. It was found that B acts as a solute (for test temperatures higher than 950°C) and segregates at the recrystallizing grain boundaries. A physical model was proposed to explain the following observations concerning the recrystallization of hot worked

austenite: i) that Nb and B can act synergistically to retard the process; and ii) that the magnitude of the retardation is not constant, but depends on the deformation conditions. The results are consistent with the hypothesis that B decreases the grain boundary diffusivity (D^{GB}) of the Nb atoms close to the grain boundaries. According to the solute drag theory, such a change increases the drag force acting on the boundary; the theory also predicts that the order of effectiveness of the substitutional alloying elements commonly found in austenite in retarding recrystallization decreases in the order: Nb > Ti > Mo > V > Mn > Cr > Ni.

Summary of the Conclusions

1) The retardation of recrystallization produced by B addition when added alone is small. However, when this retardation is compared on an atomic concentration basis, it is comparable to that produced by an equal atom fraction of Mo.

2) The simultaneous presence of Nb and B leads to the greater retardation of recrystallization than the simple sum of the retardations produced by each solute alone. Furthermore, the magnitude of this synergistic effect changes with the deformation conditions. It is a maximum at 1050, 1000 and 950°C for prestrains of 0.12, 0.25 and 0.5, respectively.

3) The rates of recovery and recrystallization under static holding conditions can be described in terms of the Avrami equation. The amount of softening preceding recrystallization is about 25 percent. The time exponent n^r for recovery has values of 0.46, 0.61 and 0.77 at predeformations of 0.12, 0.25 and 0.5, respectively, in the Nb-containing materials. The rate constant k^r depends on temperature, deformation and alloy composition. The time exponent for recrystallization n^R is approximately independent of temperature and deformation and has an average value of about 0.9. These parameters, together with the equations describing the dependence of recrystallization rate on prestrain and temperature, can be of considerable use in the computer modelling of steel rolling.

4) The increased retarding ability of B when added in the presence of Nb (at temperatures above 975°C) is due to the strain induced segregation of boron. This non-equilibrium effect results in the formation of a temporary solute atmosphere in the vicinity of the moving grain boundaries. This mode of segregation is affected by: i) the matrix diffusivity of the boron ; ii) its grain boundary diffusivity; iii) the boron-monovacancy complex diffusivity; and iv) the sweep velocity of the moving grain boundaries.

5) The synergistic interaction between Nb and B can be rationalized in terms of the influence of boron grain boundary atmospheres on the grain boundary diffusivity of Nb (D^{GB}_{Nb}) and consequently on the ratio

of the grain boundary to matrix diffusivities of Nb (D^{GB}_{Nb}/D^{M}_{Nb}). As suggested in the literature, even small amounts of interstitial impurities (20 to 40 ppm in the bulk) can reduce the grain boundary diffusivity of substitutional elements, e.g. Nb, when the former are segregated at the boundaries. According to the solute drag model of Hillert and Sundman, the reduction in the ratio D^{GB}_{Nb}/D^{M}_{Nb} produced in this way increases the drag forces exerted by the Nb on the moving boundaries.

6) Comparison of the relative differences in recrystallization rate under optimum segregation conditions clearly shows that the greatest difference corresponds to the greatest deformation. According to the model, derived in this work, this is due to the effect of deformation on the number of boron atoms transported to the boundary. Increasing the deformation increases the vacancy concentration ($\rho_v = 10^{-4 \cdot \varepsilon}$), which increases in turn the concentration of the boron-monovacancy complexes responsible for the transfer of boron to the boundaries.

7) By assuming that the effect of doping the base steel with Nb resembles that of doping pure iron with Nb, and as long as no precipitation is taking place, the solute drag model proposed by Cahn can be applied to the present experimental conditions. According to this model, at high grain boundary velocities, the element with the highest grain boundary interaction energy exerts the largest drag. Experimental evidence obtained on HSLA steels has shown that the

retarding ability of the microalloying elements increases in the following ascending order: Ni < Cr < Mn < V < Mo < Ti < Nb. Furthermore, comparison of the diffusivities of the above substitutional elements in γ-iron indicates that the strongest retarding species (Nb) is also the fastest one, followed by Ti, Mo, V, Mn, Cr, and Ni. These observations are consistent with the solute drag theory because the fastest diffusing elements are also those displaying the highest grain boundary interaction energies. Although seemingly contradictory, this is because both the interaction energy and the diffusivity increase with the extent of distortion caused by introducing a particular alloying element into a metal matrix.

8) Based on the present model for the synergistic interaction between Nb and B, boron can be predicted to display a synergism when accompanied by other alloying elements such as Ti and Mo. However, the combined effects of Ti + B or Mo + B are expected to be less than that of Nb + B because of the weaker grain boundary interaction energies displayed by these elements. Chemical and thermodynamic interactions between Nb and B may also play a role in the synergism when both of these elements are present at an austenite grain boundary; however, insufficient information is available at present to assess the importance of this contribution.

9) When B additions are made to microalloyed steels, the no-recrystallization temperature T_{nr} can be expected to be raised by up to

50°C. Thus, B-modified steels can be given greater pancaking strains than unmodified grades when rolled according to a fixed schedule. Similarly, there will be less scope for austenite grain refinement above T_{nr} unless adjustments are made to the pass sequences and temperatures. The above comments apply when a steel is cooled continuously during rolling. When processing is carried out at nearly fixed temperatures, as during some parts of seamless tube making, less non-equilibrium segregation will be produced, and the increase in T_{nr} will be less significant.

PART II EFFECT OF B ADDITION ON CARBONITRIDE PRECIPITATION IN AUSTENITE

Summary of the Method

The progress of Nb-Ti carbonitride precipitation in hot worked austenite was followed using the new method developed at McGill. This technique is based on the effect of precipitation on the stress relaxation behaviour of prestrained samples. Both prestrains of 5 and 25% were employed. The 5% prestrain was chosen so as to avoid the initiation of recrystallization during testing.

The 25% prestrain was considered to be more representative of industrial rolling practice. The samples were first reheated at 1100°C

for 30 minutes in order to ensure the dissolution of NbC and to produce an austenite grain size of about 50 μm. Following prestraining, the anvil was stopped and the process of stress relaxation was begun. During the test, the temperature was controlled to within ± 1°C, and the load was sampled continuously for up to 1 hour.

In order to study analytically the progress of precipitation during stress relaxation, samples were quenched at different stages of the process. Carbon extraction replicas were prepared from the quenched samples and the precipitates were observed and analyzed in a JEOL-100 CX electron microscope fitted with a PGT system IV energy dispersive X-ray spectrometer (EDS). The location of boron in the microstructure was studied using the technique of particle tracking autoradiography (PTA) based on the $^{10}B(n, \alpha)^{7}Li$ fission reaction with a solid detector of cellulose acetate.

Summary of the Conclusions

1) The stress relaxation technique can be used to detect niobium carbonitride precipitation in microalloyed austenite. The precipitation start and finish times correspond to breaks in the slopes of the stress relaxation curves. The stress relaxation curves also indicate when recrystallization begins, is arrested, recommences, or is terminated.

2) Employing the above method, precipitation-time-temperature (PTT) diagrams were obtained for a Nb-Ti and a Nb-Ti-B HSLA steel. The presence of B accelerates the rate of carbonitride precipitation and raises the temperatures at which such strain-induced precipitation takes place. For example, the precipitation start time decreases from 35 sec. in the Nb steel to 10 sec. in the Nb-B steel at 900°C.

3) The PTA experiments show clearly that there is an evolution in the state of the boron during the stress relaxation process. The results indicate that both cooling and deformation induce the non-equilibrium segregation of boron to the austenite grain boundaries. This segregation is gradually transformed into the grain boundary precipitation of ferroborocarbides (and some Nb borocarbides). After longer holding times, the "matrix" precipitation of Nb borocarbides takes place, mostly on dislocations and sub-boundaries.

4) The addition of boron leads to a significant increase in the concentration of interstitials in ULCB steels. This increases the concentration product of the precipitating species, thus increasing the driving force for the reaction. This appears to be one of the causes for the increased rate of precipitation of the complex Nb carbides.

5) EDX analysis of the particles contained in the extraction replicas indicates that the Nb concentration of the (Ti, Nb) precipitates increases with holding time. This supports the view that TiN particles

can act as nucleation sites for Nb carbonitride precipitation. Most of the grain boundary precipitates were shown in this way to be ferro-borocarbides and the matrix precipitates to be (Nb, Ti) borocarbides (see 3) above).

PART III THE NON-EQUILIBRIUM SEGREGATION OF BORON

Summary of the Method

After heat treatment, the boron depleted layer is removed from the surface of the samples, and the boron distribution is revealed with the aid of the particle tracking autoradiography (PTA) technique, which is based on the $^{10}B(n, \alpha)Li^{7}$ fission reaction. A cellulose film is used as a solid detector, and the film-coated samples are irradiated in a beam of thermal neutrons at integrated fluxes ranged from 0.1 to 1.4 x 10^{15} neutrons/cm^2 (at AECL, Chalk River). After etching in a strong alkaline solution and coating with chromium, the films are examined under an optical microscope. The boron sensitivity of the PTA technique used in this study is about 1 ppm, and the spatial resolution is about 2 μm.

In order to enable the characteristics of the boron distribution revealed by the PTA method to be assessed semi-quantitatively, the

samples used for measurement purposes were irradiated with the same integrated flux, 1.4×10^{15} neutron/cm^2, and the solid detector was cut from a single piece of cellulose acetate film. When different films were used, the etching times were adjusted to give etch pits of the same size. Typical size measurement results for single etch pits indicate that the average area of an etch pit is in the range 1.4 to 2.0 μm^2.

Summary of the Conclusions

1) There are two kinds of boron segregation at austenite grain boundaries. The equilibrium type forms during isothermal holding, and is particularly marked after quenching from temperatures below 700°C. Its severity decreases with holding temperature and is not sensitive to the cooling rates used in this investigation. The non-equilibrium type forms during cooling; its severity as revealed by PTA *increases* with quench temperature, in opposition to the trend displayed by the equilibrium form. Under non-equilibrium conditions, a boron depleted zone forms next to the segregated region; its width is sensitive to cooling rate.

2) The grain boundary segregation taking place during heat treatment involves the overlapping of these two kinds of segregation process. At lower temperatures, the segregation stems mainly from equilibrium considerations, whereas the non-equilibrium process becomes dominant in samples quenched from higher temperatures. The transition

temperature in the present types of steel lies in the range 650-750°C and is associated with a segregation minimum.

3) The degree of non-equilibrium segregation depends on cooling rate and quench temperature. The width X of the boron depleted zone can be used as a parameter to describe this type of segregation. The dependence of X on quench temperature T and cooling rate A is given by $X = H(T)/\sqrt{A}$, where H(T) is a function of T, as well as of composition and structure. For the present carbon-boron steels, the activation energy associated with the non-equilibrium segregation process is about 0.92 eV.

4) High temperature deformation before quenching increases the concentration of vacancies and seems to increase the concentration of vacancy-boron complexes. During cooling, the non-equilibrium segregation process is intensified by the deformation-induced increase in the complex density, but deformation does not appear to change the width of the boron depleted zone or the mechanism of the segregation process.

5) During recrystallization, two additional kinds of non-equilibrium segregation of boron can be observed. The first takes place at the original austenite grain boundaries and is attributable to the excess vacancies produced by the deformation; it develops quickly, is eliminated rapidly, and delays the recrystallization start time to a

limited degree. The second takes place at the new boundaries produced by recrystallization, and involves the sweeping of the deformed material by the boundaries. During their movement, this kind of segregation is intensified and approaches a temporarily steady level. When motion stops or at the completion of recrystallization, the segregation begins to decrease and is gradually eliminated almost entirely.

6) The synergistic effect of B and Nb can be attributed to the formation of (Nb, B) complexes. The non-equilibrium segregation of such complexes on the new boundaries increases the solute drag force, decreases the boundary velocity, and slows down the recrystallization kinetics of B-modified steels.

OVERALL CONCLUSIONS

As a result of the above work, the following general conclusions can be drawn.

1) With regard to the industrial rolling of Nb alloys, the addition of B leads to an *increase* in the pancaking temperature of 30 to 50°C. Thus, B-modified alloys receive greater pancaking strains than unmodified grades when rolled according to a fixed schedule.

2) The present results suggest that similar trends will be observed when B is added to steels containing V, Mo or Ti instead of Nb. Of these elements, V is expected to display the weakest and Ti the strongest synergistic effect (after Nb).

3) These observations can be explained by a combination of solute drag and precipitate effects. With regard to the former, B addition appears to increase the effectiveness of Nb at grain boundaries by *increasing* its matrix diffusivity. With regard to the latter, it accelerates the precipitation of carbides by increasing the concentration of the interstitial elements participating in the precipitation reaction.

4) The segregation of B to grain boundaries takes place by a number of distinct mechanisms. In addition to conventional *equilibrium* segregation, which predominates at temperatures below 750°C, there are at least three types of *non-equilibrium*, i.e. temporary, segregation that occur at temperatures between 800 and 1100°C.

5) The first type of temporary segregation is caused by cooling from preheating temperatures; it involves the migration of excess vacancies (in association with B atoms) to grain boundary sinks. A similar type of vacancy-driven segregation occurs on *isothermal* holding, when the excess vacancies are created by deformation. Finally, during recrystallization, temporary B segregation is produced by the sweeping action of the grain boundaries.

6) The usefulness of the results obtained by particle tracking autoradiography regarding the temporary segregation of B suggests that methods should be developed for studying the temporary segregation of other alloying elements in steel. One such method that shows promise is SIMS, which is currently under investigation at CANMET.

ATTACHMENTS

to Final Report on
EFFECT OF BORON ON PRECIPITATION AND RECRYSTALLIZATION KINETICS IN HOT DEFORMATION OF TITANIUM-NIOBIUM MICROALLOYED STEELS
(DSS Contract File Number: 12ST.23440-4-9057)

Mavropoulos, L. T., and Jonas, J. J. "Effect of the combined addition of niobium and boron on static recrystallization in hot worked austenite"; publication manuscript submitted to Canadian Metallurgical Quarterly; 26 pp.

He, X. L., Mavropoulos, L. T., and Jonas, J. J. "Boron segregation during the deformation and recrystallization of austenite at high temperatures"; manuscript submitted for publication in the proceedings of the International Conference on Physical Metallurgy of Thermomechanical Processing of Steels and Other Metals (THERMEC-88), The Iron and Steel Institute of Japan, Tokyo, Japan, 1988; 8 pp.

Djahazi, M., He, X. L., and Jonas, J. J. "Effect of boron on the precipitation of carbonitrides in a Nb-Ti HSLA steel"; manuscript submitted for publication in the proceedings of the Mechanical Working and Steel Processing Conference, Iron and Steel Society, AIME, Toronto, Ontario, 1987; 8 pp.

Djahazi, M., He, X. L., and Jonas, J. J. "Effect of boron on carbonitride precipitation in deformed austenite"; manuscript submitted for publication in the proceedings of the International Conference on Physical Metallurgy and Thermomechanical Processing of Steels and Other Metals (THERMEC-88), The Iron and Steel Institute of Japan, Tokyo, Japan, 1988; 7 pp.

He, X. L., Chu, Y. Y., and Jonas, J. J. "Grain boundary segregation of boron during continuous cooling"; manuscript submitted to Acta Metallurgica; 37 pp.

EFFECT OF THE COMBINED ADDITION OF NIOBIUM AND BORON ON STATIC RECRYSTALLIZATION IN HOT WORKED AUSTENITE

L.T. Mavropoulos and J.J. Jonas

Department of Metallurgical Engineering, McGill University
Montreal, Canada H3A 2A7

ABSTRACT

Four low carbon bainitic steels were compression tested under interrupted and continuous loading conditions. These materials were made from a base steel containing 0.026% C, to which were added one or both of 0.055% Nb and/or 30 ppm of B. In this way, the influence on the rapidity of recrystallization of additions of: (i) Nb; (ii) B; and (iii) Nb + B was assessed independently.

The recrystallization kinetics of the hot worked austenite were determined for prestrains of 0.12, 0.25 and 0.50 in the temperature range 900 to 1100°C. The results are presented in the form of percentage softening vs. log time plots and of RTT diagrams. The observations indicate that the addition of B is most effective in retarding recrystallization in the presence of Nb. Furthermore, the degree of retardation is influenced by both the prestrain and the temperature. The kinetics of recovery and recrystallization are characterized in terms of the Avrami equation; the influence of prestrain, temperature and alloy composition on the coefficients and exponents is described.

EFFECT OF THE COMBINED ADDITION OF NIOBIUM AND BORON ON STATIC RECRYSTALLIZATION IN HOT WORKED AUSTENITE

INTRODUCTION

An important microalloying element in the so called ultra-low-carbon-bainitic (ULCB) steels, especially from the hardenability point of view, is boron (1-10). Its effect is particularly strong in the presence of niobium (11-14). These steels owe a part of their toughness to the low carbon levels (15, 16); however, significant contributions to the impact properties can also be made by refinement of the austenite grain size prior to the bainite transformation. This is because the effective grain size for cleavage fracture in bainitic steels has a strong dependence on austenite grain size (12, 17-19), in a manner similar to that observed in the ferrite-pearlite steels. The design of rolling schedules that lead to grain refinement requires knowledge of the dependence of recrystallization rate on rolling reduction and deformation temperature (20-23). The separate roles played by the different microalloying elements in general (24), and niobium and boron in particular are also of importance in understanding the physical metallurgy of these alloys.

The aim of the present investigation was therefore to characterize the recrystallization behaviour of a series of hot worked austenites containing boron. In particular, the main objectives were:

(i) To determine the extent to which the presence of boron, alone or in conjunction with Nb, influences the rapidity of softening;

(ii) To assess the influence of a variety of prestrains and holding temperatures of industrial interest; and

(iii) To derive mathematical expressions relating the softening kinetics to the temperature and amount of the predeformation.

EXPERIMENTAL MATERIALS AND PROCEDURE

The chemical compositions of the four steels employed in the present work are given in Table 1. The low carbon content was selected as being representative of the ULCB (ultra low carbon bainitic) steels being made for pipeline applications (25, 26). The titanium addition was made to prevent boron nitride formation, which would have eliminated boron in solution, and thus have interfered with its role in promoting bainite formation. The aluminum, in turn, was added to protect the titanium from oxidation. Finally, the niobium addition was designed to provide precipitation strengthening and to improve the hardenability by acting in conjunction with the boron.

The preparation of compression specimens was based on that used in previous investigations (27-29). Cylindrical samples were machined from the as-received plates with the compression axes aligned parallel to the rolling direction. An aspect ratio (height-to-diameter) of 1.5 was selected to promote homogeneous deformation. The end surfaces of the specimens were grooved to allow for maximum retention of the glass powder lubricant. All the samples were heat treated at 1000°C for 1 hour under vacuum, and then air cooled. This normalization heat treatment was applied in order to eliminate the rolling textures present in the as-received materials; such textures frequently lead to the production of elliptical cross-sections in hot compressed samples.

The experimental technique used in this investigation for following the static recrystallization of hot worked austenite was the interrupted compression test method developed by Petkovic et al. (30). This technique is based on the principle that the yield stress at high temperatures is a sensitive measure of the structural state of the material. The degree of softening, X, taking place during the unloading period can be estimated from the expression

(1)

Here σ_m is the flow stress immediately before unloading and σ_o and σ_r are the yield stresses pertaining to the first and second cycles of loading, respectively (Fig. 1). An offset strain of 0.2% was used to define the initial flow (yield) stresses on loading and reloading. Prior to testing, the samples were austenitized at 1100°C for 15 minutes, which produced a grain size of approximately 40 μm. Then they were prestrained to equivalent strains of 0.12, 0.25 or 0.50, unloaded for increasing times and reloaded for a further deformation of 0.25 (see Fig. 1). The loading strain rate was held constant at 2 s^{-1} and test temperatures of 900, 950, 1000, 1050 and 1100°C were employed.

RESULTS

The complete fractional softening vs. holding time curves for all the experimental conditions are presented in Figures 2 to 5, where the conditions and materials employed are indicated on each diagram. Two ranges can be distinguished in all the curves: the recovery region, which corresponds to the early stages of softening (usually about 25%), and the recrystallization region (from 25 to 100% softening). The two softening processes overlap at around 25% and the transition from one mechanism to the other is marked by an acceleration of the softening process (30, 31).

In Figure 2, the amount of softening is shown as a function of the time of unloading for a prestrain of 0.25 for the Nb (open symbols) and Nb + B (full symbols) steels. It is evident from the results that: (i) the presence of boron in solution (above 950°C (32)) leads to a retardation in the rate of austenite recrystallization compared to that obtained in the unmodified niobium steel; (ii) the maximum retardation is observed at a test temperature of 1000°C; (iii) there is only limited retardation of recrystallization due to boron addition at 1100 and 900°C; and (iv) at test temperatures of 1050 and 950°C, there is an appreciable difference between the behaviours of the two steels, although the magnitude of the effect is less than that observed at 1000°C.

The softening behaviour of the base and base plus boron steels tested at 900 and 1000°C can be seen in Figure 3. For comparison purposes, the 900 and 1000°C results presented in Figure 2 for the Nb and Nb + B steels are also included. From this comparison, the following conclusions can be drawn: (i) the softening process in the base and base plus boron steels proceeds much more quickly than in the Nb and Nb + B steels; (ii) the sole addition of boron to the base steel does not appreciably retard softening; (iii) the niobium addition to the base steel causes a very large retardation; and (iv) the presence of boron in the niobium steel results in a further retardation which is larger than the sum of the retardations produced by the single additions of boron and niobium to the base steel. It is readily apparent from the above

that the combined addition of niobium and boron produces a synergistic retarding effect.

For a better understanding of this behaviour, experiments were conducted with different amounts of predeformation, namely 0.5 and 0.12. Increasing the amount of the prestrain increases the velocity of the recrystallizing grain boundaries through its effect on the dislocation density and hence the driving force. Decreasing the amount of the prestrain, by contrast, has the reverse effect.

From Figure 4 it is evident that, with increased prestrain, boron still retards recrystallization but now the effect is greatest at 950 instead of 1000°C. It is also apparent that the time for 62.5 percent softening (equivalent to 50% recrystallization because of the occurrence of about 25% softening by recovery) for the niobium plus boron steel at the temperature of greatest retardation is approximately 100 seconds, as in the previous case (Fig. 2). The softening curves also indicate that: (i) NbC precipitation begins at about 200 seconds in the Nb steel at this temperature; and (ii) the addition of boron appears to accelerate the precipitation kinetics by as much as an order of magnitude. If the precipitation did not take place at 900°C, the relative difference between the recrystallization behaviours of the Nb and Nb + B steels is expected to follow the pattern displayed in Fig. 2. (It should be added that the test technique used here is not particularly well suited to the determination of precipitation start times, and so the above values are

estimates only. More precise values concerning the present steels have been determined by stress relaxation and are presented elsewhere (32)).

The softening curves obtained from the experiments with predeformations of 0.12 (and therefore with *decreased* driving forces and grain boundary velocities) are shown in Figure 5. Once again, there is a condition of maximum retardation, at 1050°C in this case, and the time for 62.5 percent softening for the Nb + B steel is again at about 100 seconds. Furthermore, because the temperature range of these experiments is relatively high, the retarding effect is unlikely to be due to the occurrence of precipitation, but is more likely to involve some kind of solute drag process.

Strain Dependence of the Rate of Recrystallization

The effect of strain on the rate of recrystallization is depicted in Figure 6, where the results for the Nb and Nb + B steels after different prestrains are presented in the form of both softening curves (Fig. 6a) and times $t_{0.5}$ for 50% recrystallization (approximately 62.5% softening, Fig. 6b). On the latter log/log plot, the points for the various temperatures can be fitted by straight lines, the slopes of which range from about - 3.4 to - 4.0. Thus, $t_{0.5}$ can be expressed as

(2)

where A is a constant and m is the slope. Barraclough and Sellars (33) found a similar effect of strain at small strains, which they reported as

(2.1)

for C-Mn steels.

It should be noted that the above strain dependences are only valid well before the peak in the stress/strain curve is attained. Beyond the peak stress, the strain dependence decreases, dropping to zero at the onset of steady state deformation. Similarly there is a lower limit of strain to which this relationship (Eq. 2) is applicable. The data of Morrison (34), for example, indicate that it is less than 0.05 for low carbon steel at 950°C, whereas the observations of Djaic and Jonas (35) suggest a value greater than 0.055 for high carbon steel at 780°C. The above subject merits further study because low strains are frequently applied in the final passes of plate rolling and these can have significant effects on the final austenite grain size if they are in the vicinity of the critical strain for static recrystallization (22, 36).

Temperature Dependence of the Rate of Recrystallization

The qualitative effect of temperature on the rate of recrystallization was evident from the softening curves presented in Figs. 2 to 5. The temperature dependence can also be described in terms

of the time for half recrystallization ($t_{0.5}$), which is plotted against the inverse absolute temperature in Figure 7. Here data are illustrated for the plain carbon, B, Nb, and Nb + B steels submitted to a prestrain of 0.25; for comparison purposes, results for the Nb and Nb + B steels tested to prestrains of 0.12 and 0.5 are also plotted. The points for each steel and prestrain fall on straight lines, so that the recrystallization data can be expressed as an empirical equation of the form

(3)

where R is the gas constant (8.31 kJ/mole-K) and Q^R is an experimental activation energy associated with recrystallization.

It is not possible to ascribe a physical significance to Q^R because, for the "activation energy" to be strictly valid, the microstructure (particularly the dislocation density and substructure) would have to be identical at the start of each experiment carried out over the full temperature range. This can be done by using a different strain rate at each temperature so as to keep the value of $Z = \varepsilon \exp(Q/RT)$ constant (30). Due to the complexities involved, this approach was not employed in the present investigation. The measured activation energies must therefore be considered as empirical constants which simply characterize the ease of recrystallization. The average activation energies determined in this work (slopes of the lines in Fig. 7) are presented in Table 2. It can be seen that Q^R increases from 240 for the

base steel to 541 KJ/mole for the Nb + B after a predeformation of $\varepsilon_p = 0.25$. The addition of B to the base steel has a very small effect on Q^R, while that of Nb raises it by more than a factor of two.

The activation energy for the base steel is somewhat lower than a previously reported value (272 KJ/mole) (37), which can be attributed in part to the smaller initial grain sizes in this work, which are linked in turn to the influence of the TiN particles present during reheating. Finally, when the predeformation is increased from 0.12 to 0.5, the activation energies for the Nb and Nb + B steels decrease from 562 to 509 and 598 to 521 KJ/mole, respectively. This is accounted for most simply by the increase in the driving force with increased prestrain.

Recrystallization-Time-Temperature (RTT) Curves

RTT diagrams are useful to industrial metallurgists because they provide information about the start and end of softening under industrial rolling conditions (38). To signify the start and finish of recrystallization at each temperature, the amounts of 30 and 90% softening were selected from the softening curves presented above. The recrystallization start (R_s) and finish (R_f) times are displayed in Figure 8 as functions of the holding temperature. Clearly, the single addition of boron to the plain carbon steel retards the start and finish of recrystallization, but only by a small amount. The addition of Nb produces a large retardation in both the R_s and R_f times and the above

finding is, of course, in general agreement with many observations in the literature. The combined addition of Nb and B produces the greatest retardations, and these are larger than the sum of the individual retardations attributable to each element. Furthermore, the relative difference between the Nb and Nb + B steels first increases as the temperature is decreased, reaches a maximum, and then decreases again. The location of this "knee" depends on the predeformation condition, but is not associated with the process of precipitation for temperatures of 1000°C or higher (32). Nevertheless, NbC precipitation does take place at the lower temperatures, and the dashed lines in Figure 8b indicate the recrystallization kinetics expected in the absence of the deposition of second phase particles.

DISCUSSION

Modeling of the Static Softening Processes

The percentage softening versus log holding time curves presented above have a sigmoidal shape and are characteristic of processes involving nucleation and growth. The Avrami equation (39, 40)

$$x = 1 - \exp(-kt^n) \qquad (4)$$

can therefore be fitted to these results, where x is the fraction of the material recrystallized, t is the time, k is the rate constant and n is an exponent. These constants have no physical significance here due to the overlap of more than one process (recovery, recrystallization and occasionally precipitation). However, data of the present type can be used to link Avrami constants to steel chemistry, as well as to rolling parameters. By rearranging and taking logarithms, Equation 4 can be rewritten in the form:

(5)

The present data for the Nb and Nb + B steels are replotted in accordance with this relation in Figure 9, where only the points for a prestrain of $\varepsilon_p = 0.25$ and deformation temperatures of 1050, 1000 and 950°C are shown. An interesting feature of this plot is that, instead of displaying a single straight line for each steel tested at a given temperature, there are two segments to each fit. Also the slopes of the linear parts change at values of softening of about 25%. The above indicates that there are two softening processes taking place: (i) static recovery (from 0 to 25% softening) and (ii) static recrystallization (from 25 to 100% softening) (31). The values of k and n for recovery and recrystallization were therefore measured separately, by following the method introduced by Luton et al. (38).

For the analysis of recovery, it is useful to define an expression for the fractional recovery in which full recovery is represented by the reloading stress σ_∞. When only recovery is taking place, the fractional softening is given by

(6)

Here σ_m is the flow stress immediately before unloading and σ_0 and σ_r are the initial flow stresses recorded during prestraining and reloading, respectively. The superscript r is used here to denote the softening fraction attributable to recovery only. It follows that the fractional softening at the completion of recovery X^r_∞, is given by

(7)

The experimental quantities X^r and X^r_∞ can be substituted into equation (4) to yield

(8)

The values of the time exponent n^r and rate constant k^r for recovery only can be obtained from plots of $\log_{10} \ln(X^r_\infty/X^r_\infty - X^r)$ vs. $\log_{10} t$. The saturation level of X^r_∞ was chosen to be 0.25 for this purpose.

A similar approach was followed for the case of recrystallization and the equation that resulted is given by

(9)

where $X^R_\infty = 0.75$, $t_R = t - t_o$, and t_o is the time for 25% softening in this case.

The overall softening produced when the two restoration processes occur together is given by the sum of the individual components as:

$$X = X^r + X^R \tag{10}$$

Static Recovery In Figures 10a to 10c, plots of $\log_{10} \ln(X^r_\infty / X^r_\infty - X^r)$ versus log(t) are presented for the prestrains 0.12, 0.25 and 0.50, respectively. A number of observations can be made from these plots: (i) for a given predeformation, material and test temperature, the data are well represented by straight lines; (ii) the slopes of the lines (when ε_p is constant) are similar and do not depend on material chemistry or test temperature; and (iii) as the predeformation is increased from 0.12 to 0.25 to 0.50, the average slope ($\bar{n}^r$) increases from 0.46 to 0.61 to 0.77, respectively. The intersections of these lines with the vertical corresponding to $t_R = 1$ also change and the values of k^r obtained in this way increase with temperature.

Furthermore, k^r can be seen to increase from 0.33 to 0.72 to 1.40 as the predeformation of the Nb steel tested at 1000°C is increased from 0.12 to 0.25 to 0.50 (Table 3). A similar dependence of the rate constant k^r on temperature and prestrain was reported by Luton et al. (38) for ETP copper, but the numerical values were different. However, in contrast to the results of the above investigators, the time exponent n^r in the present work is not constant, but depends on the prestrain (Table 3).

The dependence of the average time exponent $\bar{n}^r$ on the prestrain is displayed in Figure 11a, and this dependence can be expressed by the following empirical formula:

$$\bar{n}^r = \varepsilon_p^{0.36} \tag{11}$$

The rate coefficient was found to depend on *both* temperature and prestrain; accordingly an empirical expression of the form

(12)

was employed in the present analysis, where $A^r(\varepsilon)$ is a constant which depends on the strain. The slopes of the ln k^r versus inverse absolute temperature curves for the Nb and Nb + B steels tested at prestrains of

0.12, 0.25 and 0.50 (Fig. 11b) provide the 'recovery' activation energies† for the two steels (Q^r_{Nb} = 193 KJ/mole and $Q^r_{Nb + B}$ = 249 KJ/mole). The intersections of the above lines with the vertical axis define in turn the pre-exponential term (A^r). By plotting ln A^r and $\log_{10}$ ln A^r versus ε_p and $\log_{10} \varepsilon_p$ (Fig. 11c), respectively, empirical expressions for ln A^r were obtained for the Nb and Nb + B steels as follows.

$$\ln A^r_{Nb} = 19.46 \cdot \varepsilon_p^{0.0645} \tag{13}$$

$$\ln A^r_{Nb + B} = 25.10 \cdot \varepsilon_p^{0.0645} \tag{14}$$

Static Recrystallization By using an approach similar to that employed for the case of recovery, $\log_{10} \ln(X^R_\infty / X^R_\infty - X^R)$ data were plotted versus $\log_{10} (t - t_o)$ for the determination of n^R (see Figure 12). Here t_o is the incubation time (time for 25% softening), values of which are illustrated in Fig. 13. The rate constants k^R obtained in this way are listed in Table 4. The only new observation which can be made here is that the average value of n^R does not vary much with predeformation and temperature and is approximately equal to 0.9. A similar overall dependence was reported by Luton et al. (38) for ETP Cu, but their value of n^R was 2.2.

---

†It should be noted that the progress of recovery is not normally described by Avrami kinetics (41). However, as the present investigation was concerned, in part, with providing rate equations for the prediction of softening rates during industrial rolling, the Avrami relation was selected from an "empirical" rather than a physical point of view. This has the advantage that the progress of both recovery and recrystallization is described by the same formalism.

The rate coefficient for recrystallization k^R was found to vary, as in the recovery case, with temperature and predeformation. It can again be related to inverse temperature and prestrain by the expression:

(15)

where the constant A^R depends on the prestrain.

From the plots of Figure 14, the values of the activation energy Q^R were determined (Q^R_{Nb} = 509 KJ/mole, $Q^R_{Nb + B}$ = 638 KJ/mole) and A^R was calculated to be

$$\ln A^R_{Nb} = 49.60 \cdot \varepsilon_p^{0.08} \quad (16)$$

$$\ln A^R_{Nb + B} = 60.30 \cdot \varepsilon_p^{0.05} \quad (17)$$

The accuracy of the above empirical expressions was tested for the Nb and Nb + B steels as follows. A test temperature of 1000°C was selected, with predeformations of 0.12, 0.25 and 0.5 at a strain rate of 2 s^{-1}. Equations 11 to 14 provided the values of the parameters n^r and k^r, from which the softening due to recovery X^r (X^r_∞ = 0.25) was estimated from Equation 8. Similarly, the softening due to recrystallization X^R (X^R_∞ = 0.75) was estimated with the aid of

Equation 9; for this purpose, Equations 15 to 17 provided the values of the parameter k^R, and Figure 13 those of the incubation time, t_o. The total softening is the sum of these two softening components (Eq. 10). In Figure 15a, the individual values of X^r and X^R are plotted, as well as the total softening X, and these are compared with the experimental data (open symbols). In addition, from Figs. 15b and 15c, it can be seen that there is good agreement between the experimental and calculated softening curves.

By means of the above analysis, the progress of static softening can be readily estimated for any holding temperature in the range 875 to 1125°C and for prestrains in the range 0.10 to about 0.60.

CONCLUSIONS

The present investigation concerned the effect of small amounts of boron (30 ppm) on the recrystallization behaviour of hot worked austenite in a plain C and a Nb steel. These tests were conducted isothermally under interrupted compression loading conditions. Prior to testing, the samples were austenitized at 1100°C for 15 minutes, after which they were prestrained to equivalent strains of 0.12, 0.25 and 0.5, unloaded for increasing times, and then reloaded for a further deformation of 0.25. The loading strain rate was held constant at 2 s^{-1} and test temperatures of 900, 950, 1000, 1050 and 1100°C were

employed. The progress of recrystallization was studied from the amounts of softening taking place during the unloading and isothermal holding intervals. The following conclusions can be drawn from this study:

1) The retardation of recrystallization produced by B addition when added alone is small. However, when this retardation is compared on an atomic concentration basis, it is comparable to that produced by an equal atom fraction of Mo.

2) The simultaneous presence of Nb and B leads to the greater retardation of recrystallization than the simple sum of the retardations produced by each solute alone. Furthermore, the magnitude of this synergistic effect changes with the deformation conditions. It is a maximum at 1050, 1000 and 950°C for prestrains of 0.12, 0.25 and 0.5, respectively.

3) The rates of recovery and recrystallization under static holding conditions can be described in terms of the Avrami equation. The amount of softening preceding recrystallization is about 25 percent. The time exponent n^r for recovery has values of 0.46, 0.61 and 0.77 at predeformations of 0.12, 0.25 and 0.5,

respectively, in the Nb-containing materials. The rate constant k^r depends on temperature, deformation and alloy composition. The time exponent for recrystallization n^R is approximately independent of temperature and deformation and has an average value of about 0.9. These parameters, together with the equations describing the dependence of recrystallization rate on prestrain and temperature, can be of considerable use in the computer modelling of steel rolling.

ACKNOWLEDGEMENTS

This work was carried out under contract to the Physical Metallurgy Research Laboratories of CANMET, Energy Mines and Resources, Ottawa. The authors acknowledge with gratitude the considerable assistance received from Dr. G.E. Ruddle, scientific administrator of the contract, in the preparation of the experimental materials and for numerous stimulating suggestions. They also express their thanks to Drs. J.M. Gray, Microalloying International, and W. Heitmann, Inland Steel, for their helpful comments and advice. Finally, they are indebted to the Canadian Steel Industry Research Association and the Natural Sciences and Engineering Research Council of Canada for scholarship support.

REFERENCES

1) W. Crafts and J.L. Lamont, "Effect of Some Elements on Hardenability", Trans. AIME 158 (1944), p. 157.

2) R.A. Grange, "Boron in Iron and Steel", Boron, Calcium, Columbium and Zirconium in Iron and Steel Alloys of Iron, Research Monograph Series, John Wiley and Sons, Inc., N.Y., N.Y., (1957), p. 3-57.

3) G.F. Melloy, P.R. Slemmon and P.P. Podgursky, Metall. Trans. 4 (1973), p. 2279.

4) Ph. Maitrepierre, D. Thivellier, J. Rofes-Vernis, D. Rousseau and R. Tricot, "Hardenability Concepts with Applications to Steel", D. Doane and J.S. Kirkaldy, ed., AIME (1978), p. 421.

5) B.M. Kapadia, Ibid., p. 448.

6) B.M. Kapadia, R.M. Brown and W.J. Murphy, Trans. AIME, 242 (1968), p. 1689.

7) C.R. Simcoe, A.R. Elsea and G.K. Manning, Trans., AIME, 203 (1955), p. 193.

8) C.R. Simcoe, A.R. Elsea and G.K. Manning, Ibid, 206 (1956), p. 984.

9) D.T. Llewellyn and W.T. Cook, Metals Tech., 1 (1974), p. 517.

10) B.J. Thomas and G. Henry, Boron in Steels, S.K. Banerji and J.E. Morral, eds., TMS/AIME, Warrendale, PA, (1980), p. 80.

11) Ph. Maitrepierre, D. Thivellier and R. Tricot, Trans. ASM, 6A (1975), p. 287.

12) B. Serin, Y. Desalos, Ph. Maitrepierre and J. Rofes-Vernis, Mém. Scient. de la Rev. de Métall., 75 (1978), p. 355.

13) G.J. Sojka, M.R. Krishnadev and S.K. Banerji, Boron in Steels, S.K. Banerji and J.E. Morral, eds., TMS/AIME, Warrendale, PA, (1980), p. 165.

14) Hiroshi Tamehiro, M. Murata and R. Habu, "Effect of Combined Addition of Niobium and Boron on Thermomechanically Processed Steel", Proc. Conf. on 'HSLA Steels '85', 4-8 November (1985), Beijing, China.

15) Y.E. Smith, A.P. Coldren and R.L. Cryderman, Towards Improved Ductility and Toughness, Climax Molybdenum Comp. Conf., Kyoto, (1971), p. 119.

16) A.P. Coldren, R.L. Cryderman and Y.E. Smith, Processing and Properties of Low Carbon Steels, AIME, (1973), p. 163.

17) J.D. Baird and R.R. Preston, Ibid., p. 1.

18) F.B. Pickering, "Microalloying 75", Union Carbide Corporation, New York, (1977), p. 9.

19) B. Mintz, R.C. Cochrane and J.D. Baird, Scandinavian Journal of Metallurgy, 1 (1972), p. 279.

20) I. Kozasu, C. Ouchi, T. Sampei and T. Okita, "Microalloying 75", Union Carbide Corporation, New York (1977), p. 120.

21) M. Cohen and W.S. Owen, Ibid., p. 2.

22) L.J. Cuddy, Metall. Trans., 12A (1981), p. 1313.

23) M. Fukuda, T. Hashimoto and K. Kunishige, "Microalloying 75", Union Carbide Corporation, New York (1977), p. 136.

24) P.J. Wray, Metall. Trans., 15A (1984), p. 2009.

25) H. Nakasugi, H. Matsuda and H. Tamehiro, Alloys for the 80's, Climax Molybdenum, (1980), p. 213.

26) I. Kozasu and K. Tsukada, Inclusions and Residuals in Steels, J.D. Boyd and C.S. Champion, eds., Ottawa, (1985), p. 119.

27) H.L. Andrade, M.G. Akben and J.J. Jonas, Metall. Trans., 14A (1983), p. 1731.

28) M.J. Luton and J.J. Jonas, Can. Metall. Quart., 11 (1972), p. 79.

29) J.E. Hockett, High Speed Testing, Vol. VI, The Rheology of Solids, p. 205. Interscience, New York, (1967).

30) R.A. Petkovic, M.J. Luton and J.J. Jonas, Acta Metall., 27 (1979), p. 1633.

31) R.A. Petkovic, M.J. Luton and J.J. Jonas, Can. Metall. Quart., 14 (1975), p. 137.

32) M. Djahazi, M.Eng. Thesis, McGill University, Montreal, (1983).

33) D.R. Barraclough and C.M. Sellars, Metal Sci., 13 (1979), p. 257.

34) W.B. Morrison, J. Iron Steel Inst., 210 (1972), p. 618.

35) R.A.P. Djaic and J.J. Jonas, Metall. Trans. 4 (1973), p. 621.

36) T.L. Mavropoulos, M.Eng. Thesis, McGill University, Montreal, (1983).

37) C.M. Sellars, "Hot Working and Forming Processes", C.M. Sellars and G.J. Davies, eds., The Metals Society, London (1980), p. 3.

38) M.J. Luton, R.A. Petkovic and J.J. Jonas, Acta Metall., 28 (1979), p. 729.

39) M. Avrami, J. Chem. Phys., 7 (1939), p. 1103.

40) M. Avrami, J. Chem. Phys., 8 (1940), p. 212; (1941), p. 177.

41) R.A. Vandermeer and P. Gordon, Recovery and Recrystallization of Metals, H. Hu, ed., Interscience Publishers, N.Y., (1962), p. 211.

BORON SEGREGATION DURING THE DEFORMATION AND RECRYSTALLIZATION OF AUSTENITE AT HIGH TEMPERATURES

X.L. He*, L.T. Mavropoulos and J.J. Jonas

Dept.of Metallurgical Engineering, McGill University,
3450 University Street, Montreal, H3A 2A7, Canada.

* On leave from Dept.of Metal Physics, Beijing University
of Iron and Steel Technology, Beijing, China.

Synopsis: The occurrence of B segregation was investigated during the recrystallization of a Nb and a Nb-free steel at 1000°C. The results indicate that the presence of B in the Nb steel leads to significant retardation of the softening process, whereas the effect of B when added alone is relatively unimportant. Two kinds of non-equilibrium segregation occur during recrystallization. The first, on the original austenite boundaries, results from the excess vacancies produced by prestraining; these lead to the precipitation of boron-vacancy and Nb-vacancy complexes on the boundaries, which leads to a delay in the recrystallization start time. The second arises from the sweeping of the deformed regions by the new boundaries. Such segregation is quickly dissipated when rapidly diffusing elements, such as B, are involved. By contrast, the segregation of slowly diffusing species, such as Nb and Nb + B complexes, is maintained for longer times, leading to much greater solute drag effects.

Key words: recrystallization; boron; non-equilibrium segregation; Nb steel; grain boundaries; autoradiography; solute drag; dislocation solute interaction; diffusion.

I. INTRODUCTION

Boron is an important microalloying element in steel because of its significant effect on hardenability. This phenomenon is usually attributed to the segregation of boron on austenite grain boundaries, a process which interferes with the nucleation of proeutectoid ferrite. The ultra low carbon bainitic (ULCB) steels, which contain B, Nb, and Ti, are based on the inhibition of ferrite formation in this way. The transformation characteristics and mechanical properties of such steels have recently been investigated by Tamehiro et al. (1,2), while the effects of boron addition on the recrystallization kinetics have been treated by Mavropoulos et al.(3). The synergistic influence of Nb-B and Mo-B in HSLA steels has also been discussed by Djahazi et al.(4) and Y.Y.Chu et al.(5), respectively. But the detailed behavior of boron addition, in particular its motion during deformation and in the course of recrystallization, remains to be clarified.

The aims of this paper were therefore threefold. (i) To investigate the characteristics of boron segregation during the deformation and subsequent recrystallization of austenite. (ii) To describe the rate of development and elimination of such deformation-induced segregation in a semi-quantitative manner. (iii) To propose a mechanism for the non-equilibrium segregation of solute atoms on moving grain boundaries.

II. EXPERIMENTAL MATERIALS AND METHODS

II-1. Experimental materials.

Four steels, two containing boron and two boron-free steels, were used in this investigation. Their detailed compositions are presented in Table I. The low carbon content was selected as being

representative of the ULCB steels. The titanium was added to prevent boron nitride formation and to control the grain size. The niobium addition was designed to provide precipitation strengthening and to improve the hardenability by acting in conjunction with the boron. The plain carbon and Nb-free boron steels were used as reference materials to establish the effect of boron addition in the absence of niobium.

Table I. Chemical Compositions of the Steels Investigated (wt.%)

	C	Mn	Si	S	P	Ti	Nb	B	Al	N
Base	0.03	1.54	0.19	0.006	0.008	0.02	-	-	0.02	0.0048
B steel	0.03	1.55	0.18	0.006	0.007	0.02	-	0.0033	0.02	0.0043
Nb steel	0.026	1.42	0.16	0.007	0.007	0.02	0.055	-	0.02	0.0063
Nb + B steel	0.026	1.56	0.15	0.007	0.006	0.02	0.055	0.0030	0.025	0.0064

II-2. Experimental method and heat treatment.

The static recrystallization experiments were conducted by means of interrupted compression testing and the percent softening taking place during the interval of unloading was estimated from the expression

$$X(\%) = 100(\sigma_m - \sigma_r)/(\sigma_m - \sigma_0) \qquad (1)$$

where σ_m is the maximum stress before unloading, and σ_0 and σ_r are the initial yield stresses during prestraining and reloading, respectively. In order to analyze the influence of boron on the recrystallization process, disc specimens, 10mm in diameter and 4mm thick, were heated to 1100°C for 10 min under an argon atmosphere. The samples were then furnace cooled to 1000°C at a cooling rate of 0.15°C/sec and austenite grain sizes of 40 to 60 μm (for the Nb and Nb-free steels) were observed. After isothermal holding for 5 min, the samples were hot compressed at a strain rate of 1 s^{-1} to a true strain of 0.25. After increasing holding times, the samples were quenched at different cooling rates (in an ice-brine mixture, water or oil), as shown in Fig.1.

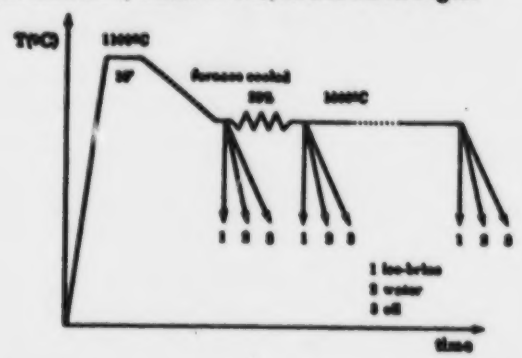

Fig.1. Schematic temperature-isothermal holding time diagram

The boron distribution was revealed with the aid of the particle tracking autoradiography (PTA) technique, which is based on the $^{10}B(n,\alpha)^{7}Li$ fission reaction. A cellulose acetate film was used as a solid detector, and the film-coated samples were irradiated in a beam of thermal neutrons to integrated fluxes of 4×10^{14} neutrons/cm^2. After etching and coating, the films were examined under an optical microscope. The boron sensitivity of the PTA technique used in this study is about 1 ppm, and the spatial resolution is about 2 μm (6).

III. EXPERIMENTAL RESULTS.

III-1. Static recrystallization and the influence of Nb and B.

The progress of softening after unloading is compared in Fig.2 for the four steels which had been deformed 25% at 1000°C. It is evident that the softening process in the plain carbon and Nb- free boron steels proceeds much more quickly than in the Nb steels. Thus addition of boron to the plain

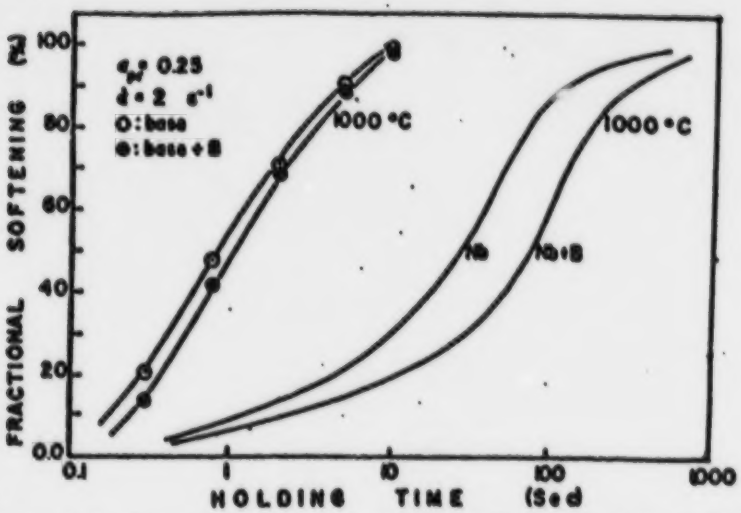

Fig.2. The softening behaviour of the plain C, C-B, Nb and Nb-B steels deformed 0.25 at 1000°C

carbon material does not appreciably retard the softening process, although it is apparent that Nb addition causes a very large retardation. In the Nb steels, the presence of boron further retards the recrystallization process, and the effectiveness of boron and niobium combined is greater than the sum expected from single additions of boron and niobium. The incubation times (t_0) and times for 50% recrystallization ($t_{0.5}$) in the four steels are summarized in Table II.

Table II. Incubation Times (t_0) and Times for 50% Recrystallization ($t_{0.5}$) in the Four Steels

	t_0 (sec)	$t_{0.5}$ (sec)
Base	0.35	1.3
B steel	0.45	1.65
Nb steel	5	38
Nb + B steel	12	98

Stress relaxation tests, which are highly sensitive to the occurrence of precipitation, were also carried out on the present materials (4). These showed that, during deformation and holding at 1000°C, no precipitation takes place in the present steels. This was confirmed by TEM analysis, and is also in agreement with the result of Fitzsimons et al. (7). Thus the retarding effect of Nb and B addition on recrystallization, under the test conditions used in this paper, can be taken to be produced by solute effects alone.

III-2. Characteristics of boron segregation during recrystallization.

The boron distribution revealed by PTA after 25% deformation at 1000°C in the carbon-boron steel is depicted in Fig.3. It can be seen that, after reheating to 1100°C and prior to deformation, the boron distribution is nearly homogeneous (Fig.3a). This indicates that there is little boron segregation of the *equilibrium* type at this temperature (i.e. at 1000°C). After deformation, the boron distribution and the degree of boundary segregation both depend on the holding time. At the very beginning of isothermal holding (less than 3 sec), there is some segregation along the original boundaries, but it is rather weak. Nevertheless, some short curved boundaries, delineating newly formed austenite grains, are outlined by bands of continuous etch pits (Fig.3b). As the holding time is increased, the amount of boundaries revealed by boron segregation develops quickly, so that after 5 sec, almost all of the boundaries have continuous etch pits associated with them (Fig.3c). As the holding time is increased from 5 to 10 sec, the degree of segregation decreases slightly and the

boundary fraction outlined by the continuous etch pits is diminished (Fig.3d). As the holding time is extended further, the boron segregation is decreased still more, and the continuous etch pits are eliminated. Finally, for times in excess of 60 sec, the boron segregation disappears completely, as shown in Fig.3f. Thus the boron segregation that develops and then disappears in Figs. 3b to 3e is clearly of the *non-equilibrium* type.

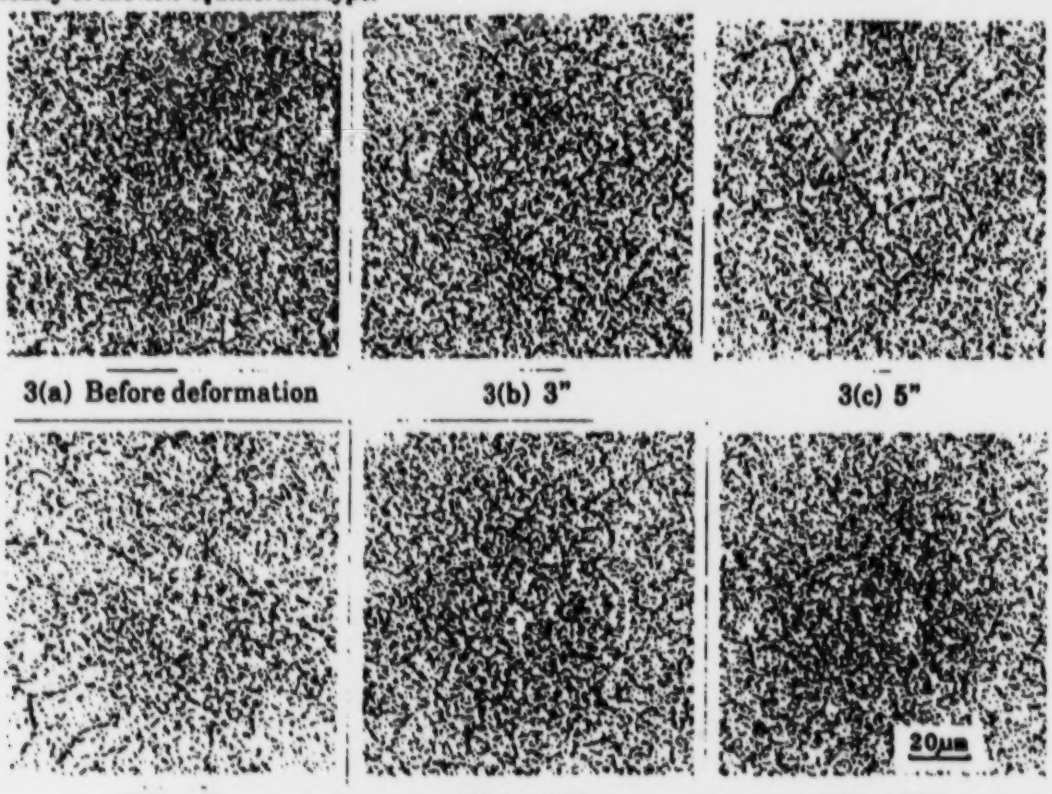

3(a) Before deformation 3(b) 3" 3(c) 5"

3(d) 10" 3(e) 60" 3(f) 150"

Fig.3. The boron distribution revealed by PTA after 25% deformation at 1000°C and different holding times in the C-B steel (quenched in ice-brine)

The changes in the boron distribution with holding time for the Nb plus B steel after 25% deformation at 1000°C are displayed in Fig.4. The general features of the development and elimination of grain boundary segregation are similar to those displayed by the carbon-boron steel in Fig.3. One of the differences, however, is that the rates of development and elimination of the strain-induced boron segregation are much slower than in the Nb-free steel. When the holding time is in excess of 600 sec, boron segregation can still be seen on some of the boundaries, as depicted in Fig.4f. Furthermore, along the newly formed austenite grain boundaries, the degree of boron segregation is more intense, and the difference in the degree of segregation between the new and original boundaries is much greater than in the carbon-boron steel, as can be seen by comparing Figs. 4b to 4f to Figs. 3b to 3e.

III-3. The rates of development and elimination of segregation.

In order to describe the evolution of grain boundary segregation during softening semi-quantitatively, the degree of segregation was measured as a function of holding time. For this purpose, a parameter $K = L/L_M$ was defined, where L is the total length of continuous etch pitting along the boundaries per unit area at a particular time and L_M is the maximum value of L attained during the entire softening process. It should be noted that the total length of grain boundary L_0 varied with the holding time during softening; at the maximum value of L, L_M/L_0 was about 85% for the carbon-boron steel and 95% for the Nb-B steel, respectively. The dependences of K on holding time for the B and Nb-B steels are shown in Fig.5, from which it can be seen that the segregation maximum appears at about 5 and 100 sec, respectively.

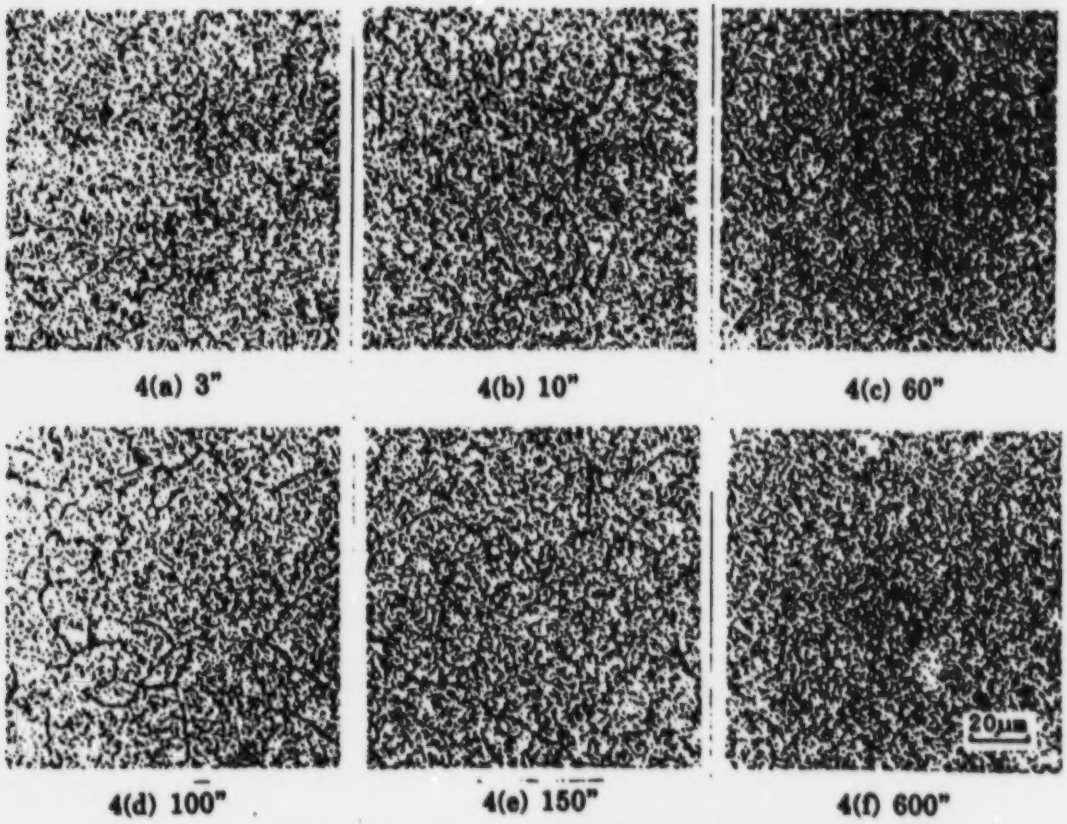

4(a) 3" 4(b) 10" 4(c) 60"

4(d) 100" 4(e) 150" 4(f) 600"

Fig.4. The boron distribution revealed by PTA after 25% deformation at 1000°C and different holding times in the Nb-B steel (quenched in ice-brine)

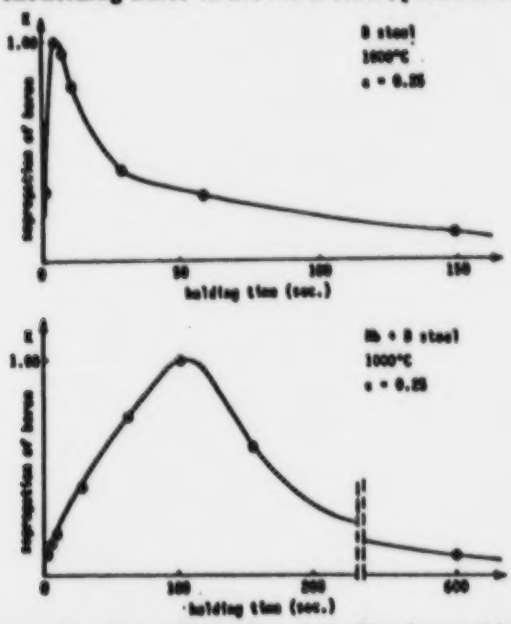

Fig.5. Segregation factor K as a function of isothermal holding time after deformation at 1000°C for the B and the Nb-B steels

III-4. Boron segregation along moving grain boundaries.

The non-equilibrium segregation revealed by PTA in the samples quenched after different times can be described as being of two types. The segregation that develops on the original boundaries at the beginning of holding results from the excess vacancies produced by prestraining. At the high temperatures used in this study, it is rather weak and is quickly eliminated (Figs.3b and 4a). The second type of segregation takes place on the *new* boundaries produced by recrystallization, (see, for example, Fig.6a for the Nb-B steel after deformation and 10 sec. of holding). When the new grains begin to grow, this kind of segregation is intensified and develops to a degree which is much greater than that on the original boundaries. For example, in the Nb-B steel quenched in ice-brine after deformation and held for 60 sec, the segregation on the moving boundaries (labelled A) can be seen much more clearly than on the original boundaries, on which the etch pit bands are no longer visible (Fig.6b). When a similar sample is quenched in oil, the non-equilibrium segregation of boron that takes place during cooling affects *all* the boundaries (new and original), as illustrated in Fig.6c. In this case, the location and shape of the new boundaries, and the relationship between the new and the original boundaries (labelled B) are clearly evident. The experimental results also indicate that segregation on moving boundaries persists for appreciable times, being maintained until boundary impingement occurs (as in Fig.6d), after which this kind of segregation begins to decrease gradually.

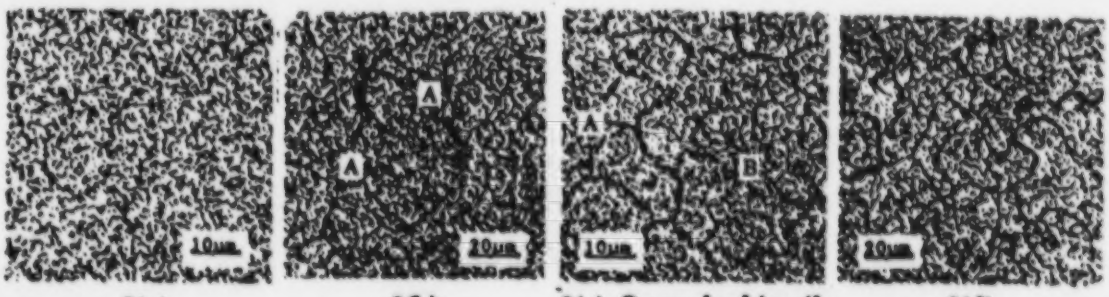

6(a) 6(b) 6(c) Quenched in oil 6(d)

Fig.6. The distribution along moving grain boundaries revealed by PTA after 25% deformation at 1000°C in the Nb-B steel (quenched in ice-brine or oil)

In the carbon-boron steel, this phenomenon has the same features, but the degree of segregation along the moving boundaries is weaker and the rate of elimination is faster than in the Nb-B steel.

IV. DISCUSSION.

IV-1. The deformation induced segregation of boron.

After hot deformation, two kinds of non-equilibrium segregation can occur. The first is similar to the segregation produced during cooling (8,9) in that it results from the presence of excess vacancies. Deformation increases the concentration of vacancies and therefore of boron-vacancy complexes in the matrix. During holding, these vacancy complexes are annihilated at the grain boundaries, sub-boundaries and dislocations, leading to the non-equilibrium segregation of boron. During high temperature deformation, boron diffusion is relatively rapid, and the excess vacancy concentration is not particularly high, so that dynamic segregation phenomena of this type are quite weak. Some preliminary results obtained on a Mo-B steel quenched from 1200 to 1000°C (9) indicate that this kind of segregation is eliminated almost completely after 20-30 sec. This process is therefore most likely to affect the nucleation rather than the growth stage of recrystallization.

The non-equilibrium segregation of boron on *moving* boundaries involves the annihilation of boron-containing dislocations at the boundaries. This is because there is a characteristic local volume change δV around a solute atom if the sizes of solute and matrix atoms are different. The size difference leads in turn to an interaction energy $U = p\delta V$ between a dislocation with an internal stress field p and the solute atom. The solute concentration (C) in local equilibrium in the presence of p is thus

$$C/(1-C) = (C_0/(1-C_0))\exp(U/KT) \qquad (2)$$

where C_0 is the bulk equilibrium concentration of the solute. As T is increased, the ratio C/C_0 decreases, but is always greater than 1. During deformation, the dislocation density increases by several orders of magnitude, after which large numbers of solute atoms tend to move to the dislocations and to decrease the strain energy of the matrix.

When the recrystallization process begins, the new grain boundaries will move towards the high dislocation density areas, and leave regions with low dislocation densities behind them. The annihilation of large numbers of dislocations on these boundaries thus leads to the deposition of the atmospheres of solute atoms associated with the dislocations at the boundaries. During recrystallization, non-equilibrium segregation will occur if the new boundaries do not move too slowly or too quickly. A temporarily stable level of segregation is attained when the number of solute atoms drawn into the boundaries by the dislocations is equal to the number leaving by diffusion. Such segregation is gradually eliminated by solute diffusion when movement of the new boundaries stops because of impingement or for other reasons.

IV-2. The synergistic effect of Nb and B on recrystallization.

The mechanism of non-equilibrium segregation on moving boundaries during recrystallization described above is applicable to several kinds of solute atom, as long as these interact strongly with dislocations and grain boundaries. The results of this investigation (especially the PTA observations) indicate that boron segregates to the new boundaries produced during recrystallization. Some recent reports in the literatures suggest that Nb also belongs to this class of element (10). The relative effectiveness in retarding recrystallization of the non-equilibrium segregation to grain boundaries of these two elements will then depend on how long such temporary segregation can be maintained.

At the temperature of 1000°C used in this study, the diffusivities of B and Nb are about 5.2×10^{-7} and 1.01×10^{-11} cm^2/sec (11,12), leading to B and Nb atom velocities of about 10.2 and 0.045μm/sec. From the kinetics of recrystallization at 1000°C and the average austenite grain sizes (60 and 40μm for the carbon-boron and Nb steels, respectively), the new boundary velocities can be estimated to be about 7.5 and 0.29 μm/sec for the two steels. It is therefore clear that, under the present conditions, the segregation of boron (when added alone) is not stable and will be eliminated relatively rapidly. Furthermore, the boron atoms can move more quickly than the new boundaries, so that the retarding effect of this kind of boron segregation is not expected to be significant. By contrast, the Nb atoms move much more slowly, so that the Nb segregation formed during new boundary movement will have a much larger effect on their velocities.

The results also indicate that the simultaneous presence of Nb and B retards recrystallization more effectively than expected from the sum of the effects of single additions of B and Nb. Turning to the Nb-B phase diagram, it is evident that Nb and B can form several compounds. Also the atomic radii R_{Fe}, R_{Nb} and R_B are 1.274, 1.468 and 0.97Å, respectively, so that $(R_{Nb} + R_B)/2$ is nearly equal to R_{Fe}. Thus Nb and B have a strong tendency to form Nb-B complexes, decreasing the distortion energy of the lattice in this way. During recrystallization, the non-equilibrium segregation of B and Nb to the new boundaries is expected to take place. According to the solute drag theory (13), the drag force increases with D_M (impurity matrix diffusivity). If the diffusivity of the Nb+B complex is higher than that of Nb, the drag force will increase accordingly, leading to the greater retardation of recrystallization.

V. CONCLUSIONS

1. The addition of boron to a Nb steel retards the recrystallization of austenite at 1000°C to a significant degree. By contrast, the effect of boron when added alone is not of commercial importance.

2. During recrystallization, two kinds of non-equilibrium segregation of boron can be observed. The first takes place at the original austenite grain boundaries and is attributable to the excess vacancies produced by the deformation; it develops quickly, is eliminated rapidly, and delays the recrystallization start time to a limited degree. The second takes place at the new boundaries produced by recrystallization, and involves the sweeping of the deformed material by the boundaries. During their movement, this kind of segregation is intensified and approaches a

temporarily steady level. When motion stops or at the completion of recrystallization, the segregation begins to decrease and is gradually eliminated almost entirely.

3. The synergistic effect of B and Nb can be attributed to the formation of (Nb,B) complexes. The non-equilibrium segregation of such complexes on the new boundaries increases the solute drag force, decreases the boundary velocity, and slows down the recrystallization kinetics of B-modified steels.

ACKNOWLEDGMENTS

The authors acknowledge with gratitude the financial support received from the Natural Sciences and Engineering Research Council of Canada, the Canadian Steel Industry Research Association (CSIRA), and the Ministry of Education of Quebec (FCAR program). The authors are also indebted to Dr. G.E. Ruddle, of PMRL, CANMET, for his encouragement and support and for initiating this program.

REFERENCES

1) H.Tamehiro, M.Murata, R.Habu and M.Nagumo: Trans. ISIJ, 27(1987), 120.

2) H.Tamehiro, M.Murata, R.Habu and M.Nagumo: Trans. ISIJ, 27(1987), 130.

3) T.Mavropoulos, J.J.Jonas and G.E.Ruddle: Proc. Int. Conf. on HSLA Steels'85, 4-8, Nov.1985. HSLA Steels: Metallurgy and Applications. Eds. J.M.Gray et al. ASM, 1986, 229.

4) M.Djahazi, X.L.He and J.J.Jonas: Int. Symp. on Microstructure and Properties of HSLA Steel, 3-5 Nov.1987. Pittsburgh, U.S.A.

5) Y.Y.Chu, X.L.He, Z.X.Zhou and T.Ko: Proc. Int. Conf. on HSLA Steel'85, 4-8, Nov.1985. HSLA Steels: Metallurgy and Applications. Eds. J.M.Gray et al. ASM, 1986, 351.

6) X.L.He and Y.Y.Chu: J. Phys. D: Appl. Phys., 16(1983), 1145.

7) G.Fitzsimons, K.Tiitto, R.Fix, and A.J.DeArdo: Metall.Trans., 15A(1984), 241.

8) T.H.Williams, A.M.Stoneham and D.R.Harries: Metal Sci., 10(1976), 14.

9) X.L.He, Y.Y.Chu, L.Tang, Z.X.Zhou and T.Ko: Proc. Int. Symp. on Grain Boundary Structure and Related Phenomena, Minakami Spa, Japan, 25-29 Nov. 1985.

10) M.G.Akben, I.Weiss and J.J.Jonas: Acta Metall., 29(1981), 111.

11) P.E.Busby, M.E. Warge, C and.Wells: J.Met., 5(1953), 1463.

12) B.Sparke, D.W.James and G.M.Leak: J.Iron Steel Inst., 203(1965), 152.

13) M.Hillert and B.Sundman: Acta Metall., 24(1976), 731.

EFFECT OF BORON ON THE PRECIPITATION OF CARBONITRIDES IN A Nb-Ti HSLA STEEL

M. Djahazi, X.L. He* and J.J. Jonas

Department of Metallurgical Engineering, McGill University, Montreal, Canada

* Beijing University of Iron and Steel Technology, China

ABSTRACT

The progress of Nb-Ti carbonitride precipitation in hot worked austenite was followed using the new mechanical method developed by Liu. This technique is based on the effect of precipitation on the stress relaxation behaviour of a 5% prestrained sample. Precipitation-time- temperature (PTT) curves were determined using this technique on a Nb-Ti and a Nb-Ti-B steel. Samples were helium quenched at different stages of stress relaxation and the precipitates were analyzed by means of carbon extraction replication. The influence of 30 ppm boron on the precipitation process was assessed with the aid of particle tracking autoradiography (PTA). The results indicate that boron addition *accelerates* carbonitride precipitation, and that borocarbide precipitation, which is still more rapid, occurs primarily at the austenite grain boundaries.

INTRODUCTION

The beneficial effect of boron addition in steel has been recognized for a long time (1,2). Of greatest interest is its effect on the hardenability, as the addition of only a few ppm increases it substantially. Thus boron addition is an effective alternative to other more expensive hardenability agents, such

as Mo, Cr and Ni . The presence of boron also modifies the γ-to-α transformation (3), and improves the creep resistance (4), formability (5), and hot workability (6). Nevertheless, a lack of reproducibility of the boron effect has led to several investigations aimed at a better understanding of the mechanisms by which boron plays its role (7-13).

Boron has been used extensively in quenched and tempered steels (14). It has also been employed in controlled rolled and ultra low carbon bainitic steels (ULCB), used mainly for large diameter pipelines (15). In these materials, the simultaneous presence of Nb, Ti and boron produces an excellent combination of strength, toughness and weldability.

As boron has been studied mainly in quenched and tempered steels, only limited data are available regarding its behaviour under controlled rolling conditions (16,17), or its effect on the precipitation of carbonitrides (4,18,19). For this reason, the influence of boron on the recrystallization and precipitation kinetics of a series of ULCB steels is under investigation in McGill's hot working laboratories. The recrystallization part of this study is now complete (20), and we present here some of the results pertaining to the effect of boron on carbonitride precipitation.

EXPERIMENTAL MATERIALS AND METHOD

The materials investigated consisted of a base steel containing 0.026 wt% carbon to which one or both of 0.055% Nb and 30 ppm boron were added. Their detailed chemical compositions are listed in Table I. The steels were prepared at the Physical Metallurgy Research Laboratories of the Department of Energy, Mines and Resources, Ottawa and were subsequently machined into compression cylinders 11.9 mm high and 7.9 mm in diameter. The specimens were given a prior heat treatment at 1000 °C for 3 hours followed by air cooling in order to eliminate the rolling texture in the as-received plate.

The samples were solutionized at 1100 °C for 30 minutes in order to ensure the dissolution of NbC and to produce an austenite grain size of 50 μm.

The experiments were carried out on a computerized MTS testing machine set up for hot compression at constant true strain rates. A vacuum furnace was employed to produce the required high temperatures, which were controlled from a thermocouple placed adjacent to the sample. The sample ends were grooved and powdered glass lubricants were used in order to reduce the friction between the faces of the sample and the compression tooling.

After solution treatment, each specimen was immediately cooled to the test temperature by shutting off the furnace; under these conditions, the mean cooling rate is 2 °C/s. Once the test temperature was attained, the samples were held for 1 min. to ensure that the temperature was fairly uniform before a 5 pct prestrain was applied at a true strain rate of 0.1 s^{-1} . The 5 pct prestrain was chosen so as to avoid the initiation of recrystallization during testing. Following the prestraining, the anvil was stopped and the process of stress relaxation was begun. During the test, the temperature was controlled to within ± 1 °C, and the load was sampled continuously for up to 1 hour.

The details of this method developed by Liu and Jonas are described elsewhere (21). In order to study analytically the progress of precipitation during stress relaxation, samples were quenched at different stages of the process. Carbon extraction replicas were prepared from the quenched samples and the precipitates were observed and analyzed in a JEOL-100 CX electron microscope fitted with a PGT system IV energy dispersive X-ray spectrometer (EDS). The location of boron in the microstructure was studied using the technique of particle tracking autoradiography (PTA) based on the $^{10}B(n,\alpha)^{7}Li$ fission reaction with a solid detector of cellulose acetate (22).

RESULTS AND DISCUSSION

1.Mechanical testing

The relaxation data obtained on the Nb-Ti-B and Nb-Ti steels at 850 and 870°C are shown in Figures 1 to 4. It is apparent that the stress vs log (time) dependencies of the Nb-Ti-B and Nb-Ti steels are similar for the first 10 seconds. After this time, the slopes of the stress vs log time curves begin to change, suggesting that precipitation is occurring during relaxation. About 30 seconds after prestraining, the progress of stress relaxation is almost stopped. The two curves remain parallel until there is a second change of slope and then the stress drops continuously until the end of the test. The starting and terminating points of the plateaus can be identified as the precipitation start (Ps) and precipitation finish (P_f) times (21), as indicated by the arrows in Figures 1 and 2. Stress relaxation data of this type were collected over the temperature range 800-950°C.

The results indicate that, as the test temperature is increased, the break in slope becomes more difficult to observe; it disappears entirely at 950°C. At this temperature, the equilibrium volume fraction of the precipitates is close to 3.5×10^{-4} and this indicates that the method is no longer valid when the volume fraction of precipitate is smaller than this value. Also, no tests were conducted at temperatures below 800°C because the γ-to-α transformation was taking place. Figure 5 shows the PTT diagram for the Nb-Ti and Nb-Ti-B steels obtained by plotting the precipitation start and finish times from the stress relaxation data versus temperature. For both steels, the PTT curves are C-shaped, with the nose for the Nb-Ti-B steel at around 830°C and 12 seconds, while for the Nb-Ti steel it is at around 800°C and 18 seconds. These results indicate that the presence of boron in hot deformed austenite accelerates the precipitation of carbonitrides and enables them to appear at higher temperatures.

2.Electron microscopy

The electron microscopy investigation had two major aims: first, to verify the validity of the stress relaxation technique as far as the

precipitation of niobium carbonitride is concerned, and second to determine the distribution, size and composition of the precipitates formed during the relaxation process. The examination of carbon extraction replicas showed that either no or very few precipitates are present prior to deformation and during the early stages of stress relaxation. As the holding time is increased, the precipitate size distribution changes. Four main kinds of precipitates were found: (Ti Nb) (C,N), Nb(C,N), $Fe_{23}(C,B)_6$ and TiN. The presence of complex TiNb precipitates in deformed austenite has already been reported (23). Only a few precipitates containing Nb alone (without any Ti) were found, and the precipitates had complex compositions. This indicates that fine TiN or TiNbN particles can act as nucleation sites, leading finally to TiNb(C,N) precipitates. Iron rich precipitates were found only at grain boundaries; they were present in greater numbers in the Nb-Ti-B steel, indicating that the addition of boron accelerates and favours the precipitation of this kind of compound. In Figures 6 and 7 are shown selected electron micrographs of the precipitates observed in samples quenched after various times during stress relaxation.

3.Particle tracking autoradiography

It was of interest to study the location of boron and the distribution of boron compounds during the various stages of these tests. Samples were quenched at 850°C and studied by means of this technique. Some of the results pertaining to this test temperature are illustrated in Figure 8. They indicate that, after solutionizing, there is a homogeneous distribution of boron in the steel. By contrast, when the samples are cooled from 1100 to 850°C, the grain boundary segregation of boron is induced. As the holding time is increased, the degree of segregation at austenite grain boundaries is weakened, leading to boron containing precipitates. Other results not presented here also reveal that boron segregation takes place at subgrain boundaries. Further details of the microstructural aspects of this investigation will be published elsewhere in more complete form (24).

CONCLUSIONS

1. The stress relaxation technique can be used to detect niobium carbonitride precipitation in microalloyed austenite. The precipitation start and finish times correspond to breaks in the slopes of the stress relaxation curves.
2. Employing the above method, precipitation-time-temperature (PTT) diagrams were obtained for a Nb-Ti and a Nb-Ti-B HSLA steel . The presence of B accelerates the rate of carbonitride precipitation and raises the temperatures at which such precipitation takes place.
3. PTA experiments show clearly that there is an evolution in the state of boron during the stress relaxation process. This evolution could provide the basis for an explanation of the mechanism by which boron affects the precipitation process.

REFERENCES

1. T.W. Lippert, "Boron", Iron Age, Vol. 19, (1942).
2. L.J. Rohl, JISI, Vol. 176, p. 173, (1954).
3. G.J. Sojka, M.R. Krishnadev and S.K. Banerji, "Boron in Steel", eds. S.K. Banerji and J.E. Morral, AIME, Warrendale, PA, p. 165, (1980).
4. B.J. Thomas and G. Henry, Ibid., p. 80.
5. G.S. Hauser, "Cold forming techniques-and how applications could be expected by more suitable steels", J. Metals, p. 969, Sept. (1965).
6. R.A. Grange, "Boron in Iron and Steel", Research Monograph Series, John Wiley and Sons Inc., N.Y.,.p. 35, (1957).
7. G. Henry and J. Philibert, Mem. Sci. Rev. Metall., Vol. 4, p. 233, (1970).

8. B.M. Kapadia, R.M. Brown and W.J. Murphy, Trans. AIME, Vol. 242, p. 1689, (1968).
9. M. Uneo and T. Inoue, Trans. ISIJ, Vol. 13, p. 210, (1973).
10. G.F. Melloy, P.R. Slimon and P.P. Podgursky, Met. Trans, Vol. 4, p. 2279, (1973).
11. A. Brown, J.D. Garnish and R.W.K. Honeycombe, Met. Sci. Vol. 8, p. 317, (1974).
12. R.A. Grange and J.B. Michell, Trans. ASM, Vol. 53, p. 157, (1956).
13. "Boron in Steel", eds. S.K. Banerji and J.E. Morral, AIME, Warrendale, PA, (1980).
14. R. Habu, M. Miyata, S. Sekino and S. Goda, Trans. ISIJ, Vol. 18, p. 492, (1978).
15. H. Nakasugi, H. Matsuda and H. Tamehiro, "Alloys for the 80's, Climax Molybdenum, Ann Arbor, p. 213, (1980).
16. B. Serrin, Y. Desalos, Ph. Maitrepierre and J. Rofes-Vernis, Mem. Sci. Rev. Met., Vol. 75, p. 355, (1978).
17. S. Watanabe, H. Ohtani and T. Kunitake, Tetsu-to-Hagané, Vol. 62, p. 1842, (1976).
18. H. Tamehiro, M. Murata, R. Habu and M. Nagumo, Trans. ISIJ, Vol. 27, p. 120, (1987).
19. H. Tamehiro, M. Murata, R. Habu and M. Nagumo, Trans. ISIJ, Vol. 27,p. 130, (1987).
20. T. Mavropoulos, J.J. Jonas and G.E. Ruddle, "HSLA Steels :Metallurgy and Applications", Proc. Int. Conf. on HSLA Steels'85, eds. J.M. Gray, T. Ko, S. Zhang, B. Wu and X. Xie, ASM, p. 229, (1987).
21. W.J. Liu and J.J. Jonas, ibid., p. 253.
22. X.L. Hé and Y.Y. Chu, J. Phys. D: Appl. Phys. Vol. 16, P. 1145, (1983).
23. D.C. Houghton, G. Weatherly and J.D. Embury, "Thermomechanical Processing of Micro-alloyed Austenite", eds. P.J. Wray and A.J.DeArdo, AIME, Warrendale, PA, p.267, (1982).
24. M. Djahazi, X.L. Hé and J.J. Jonas, to be published.

Table I - Chemical Composition in wt. pct. of the Steels Tested

Steel	C	Mn	Si	P	S	Ti	Nb	B	Al	N
Nb-Ti	.026	1.42	.156	.006	.007	.02	.055	----	.02	.0063
Nb-Ti-B	.026	1.56	.150	.006	.007	.02	.055	.003	.025	.0064

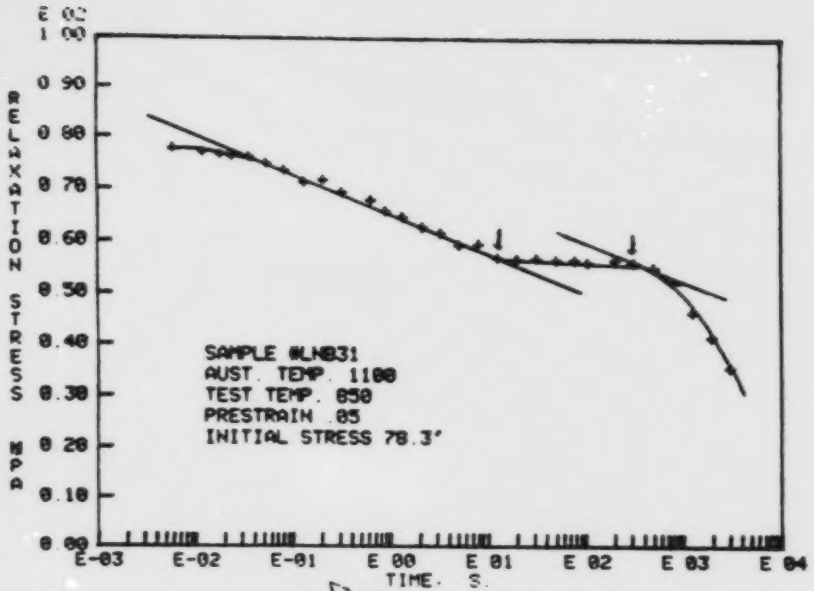

Fig. 1

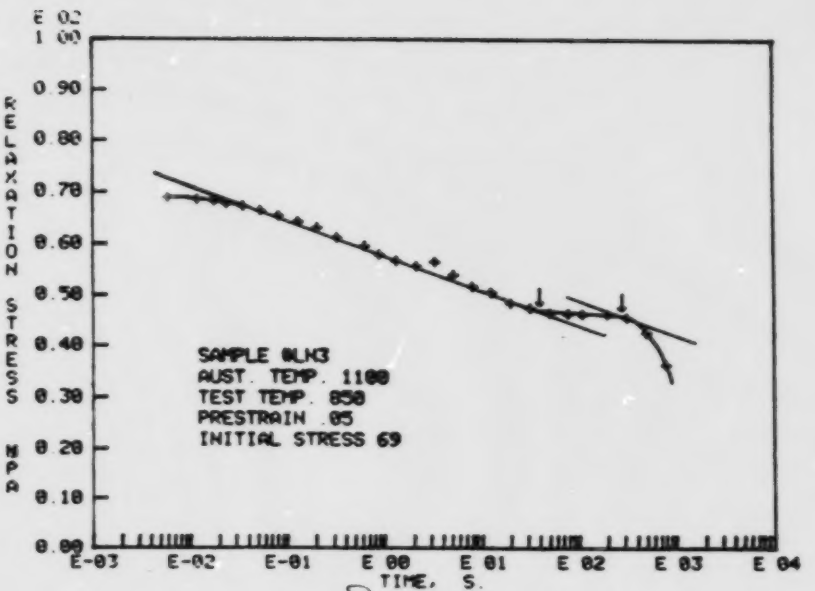

Fig. 3

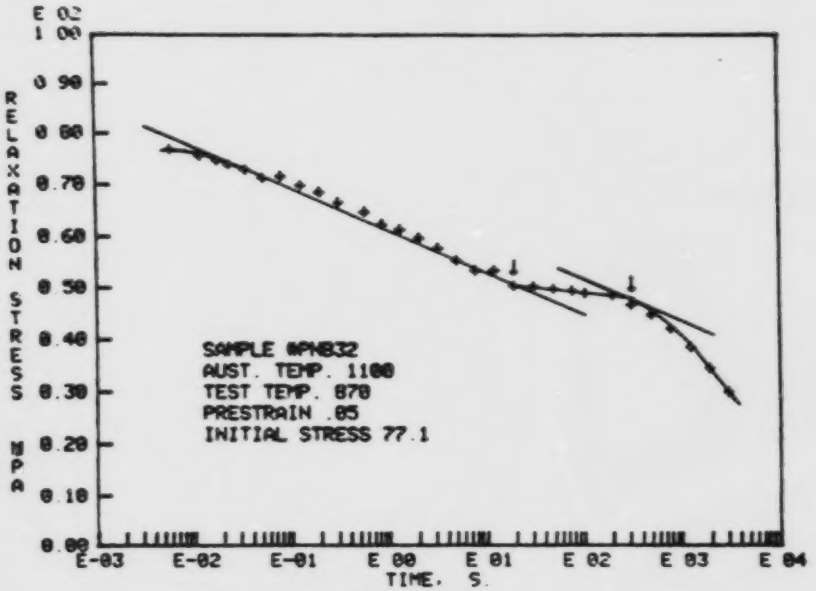

Fig. 2

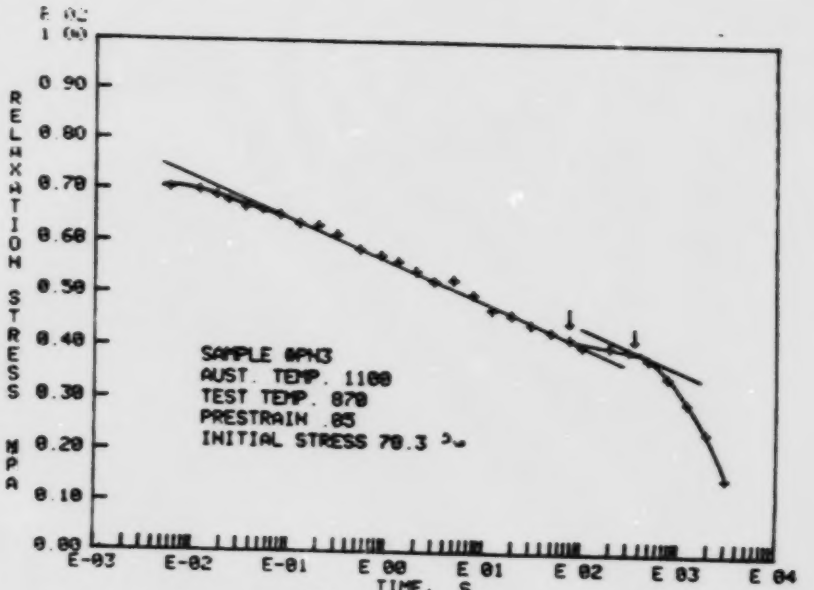

Fig. 4

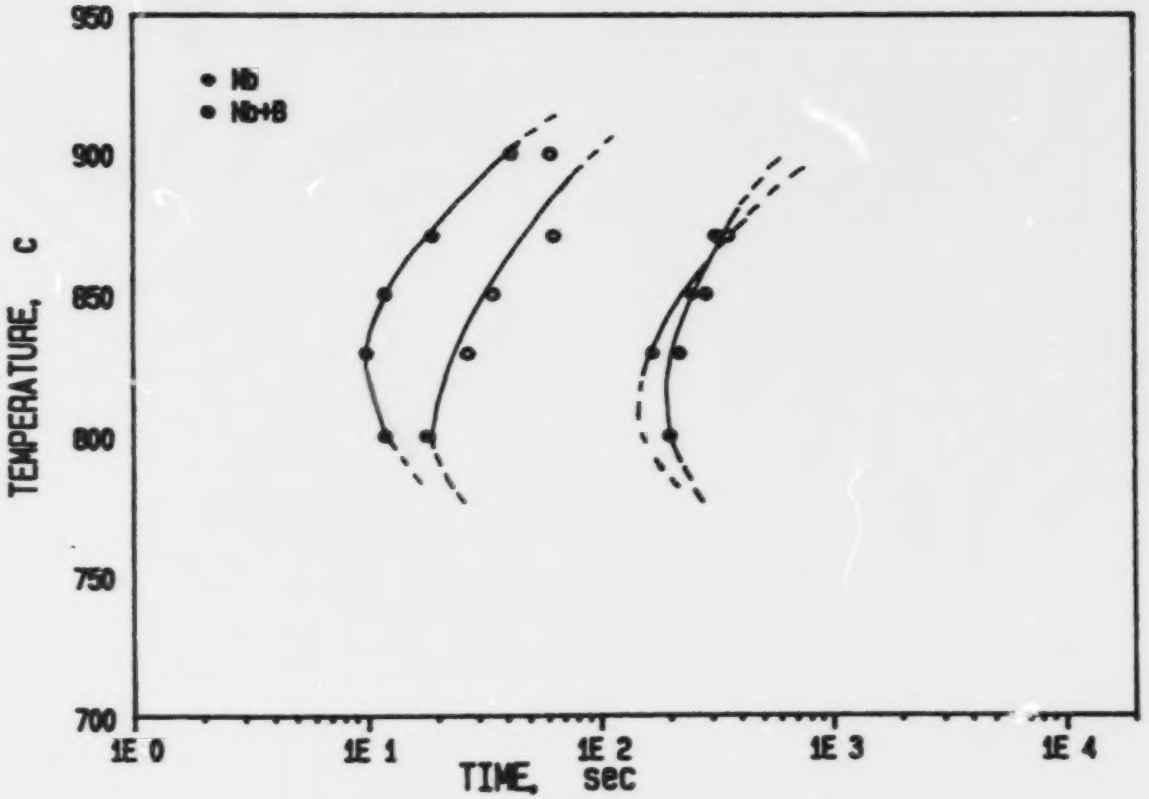
950
900
850
800
750
700
• Nb
• Nb+B
TEMPERATURE, C
1E 0
1E 1
1E 2
1E 3
1E 4
TIME, sec

Fig. 5

fig. 6

b)

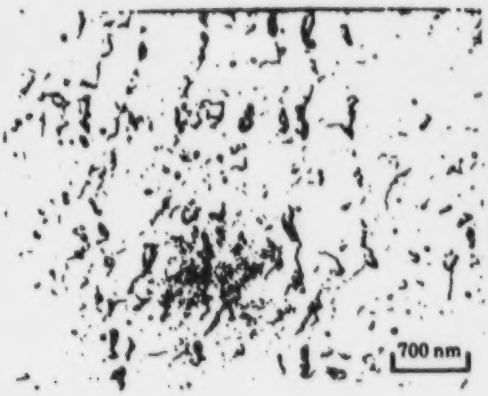

a)

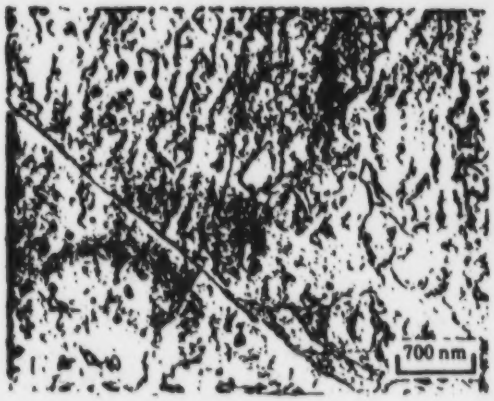

fig. 7

b)

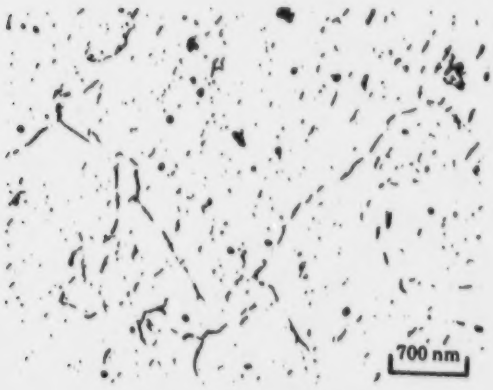

a)

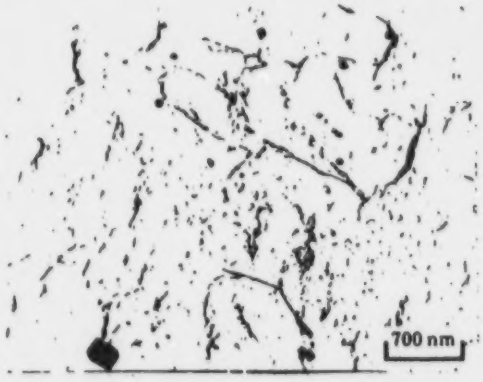

fig. 8

b)

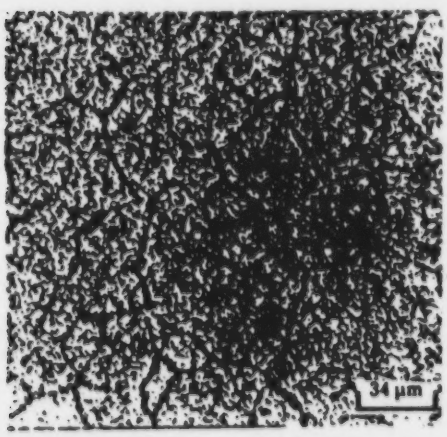

a)

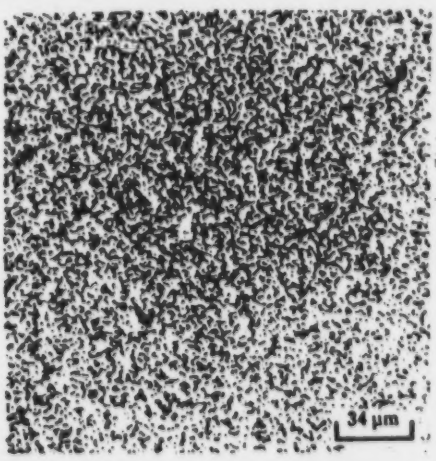

d)

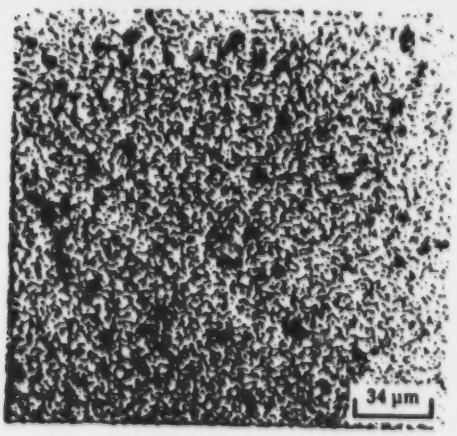

c)

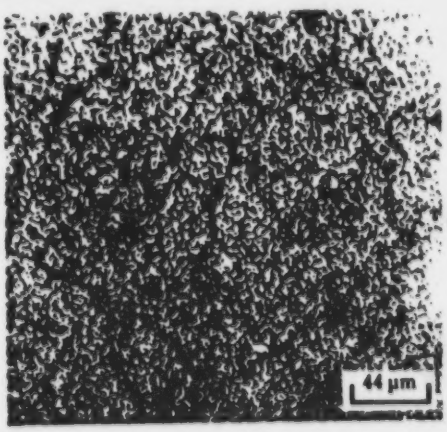

EFFECT OF BORON ON CARBONITRIDE PRECIPITATION IN DEFORMED AUSTENITE

M.Djahazi, X.L.He* and J.J.Jonas

Dept. of Metallurgical Engineering, McGill University
3450 University Street, Montreal, H3A2A7, Canada

* On leave from Dept. of Metal Physics, Beijing University of Iron and Steel Technology, China

Synopsis: The influence of boron on carbonitride precipitation was studied in a Nb-B and a B-free Nb steel. High temperature stress relaxation tests were used to follow the progress of precipitation in these two materials. The results show that the addition of boron to a Nb steel accelerates carbonitride precipitation and significantly retards recrystallization. The non-equilibrium segregation of these two elements to austenite grain boundaries and dislocations is one of the factors responsible for this effect; the other is the increase in the interstitial concentration, which raises the driving force for precipitation.

Key words: boron; carbonitride precipitation; borocarbide precipitation; non-equilibrium segregation; recrystallization; stress relaxation.

I. INTRODUCTION

The effect of the addition of boron to steels has long been recognized as important, mainly with respect to the hardenability of heat treatable grades (1). In recent years, in response to the growing demand for inexpensive, strong, tough and weldable alloys, ultra low carbon bainitic (ULCB) steels containing B, Nb and Ti have been developed. Several investigations have been undertaken to determine the optimum chemical composition and thermomechanical processing conditions for these materials (2,3). However, only limited studies (4) have been concerned with the effect of boron addition on the precipitation behaviour of carbonitrides in general and its influence under rolling conditions in particular.

In this paper, some results are described pertaining to the effect of 30 ppm boron on recrystallization and precipitation in deformed ULCB austenite. Other aspects of this work dealing particularly with the recrystallization behaviour (5) and with the non-equilibrium segregation of boron (6) have been presented elsewhere.

II. EXPERIMENTAL TECHNIQUES AND ALLOYS

II-1. Experimental procedure

A computerized MTS machine set up for hot compression at constant true strain rates was used. Each specimen was austenitized at 1100 °C for 30 minutes and then cooled to the test temperature by shutting off the furnace; this led to a mean cooling rate of about 2 °C/sec . Once at the test temperature, the sample was held for one minute so that temperature homogeneity within the sample could be attained. After equalization, it was deformed 5% at a true strain rate of 0.1 s^{-1} or 25% at a true strain rate of 1 s^{-1}. The 5% prestrain was chosen in order to avoid recrystallization during subsequent holding. Test temperatures of 800, 830, 850, 870, 900, 950 and 1000 °C were employed. After deformation, the anvil was stopped and the process of stress relaxation was begun.

By quenching the samples at different stages of the test, it was possible to follow the progress of precipitation during stress relaxation (7). A JEOL-100 CX electron microscope fitted with a PGT system IV energy dispersive X-ray spectrometer (EDS) was used to observe and analyse the precipitates removed from the sample by the carbon extraction replication technique. Finally, the

method of particle tracking autoradiography (PTA), which is based on the 10B(n, α)7Li fission reaction, was employed to study the location of the boron in the microstructure (8).

II-2. Steels

The experimental materials were prepared at the Physical Metallurgy Research Laboratories of the Department of Energy, Mines and Resources, Ottawa. Their detailed chemical compositions are presented in Table I. Cylindrical samples about 11.9 mm high and 7.9 mm in diameter were cut from the central regions of the as-received hot rolled plates. A prior heat treatment was given to the samples in order to eliminate the rolling texture present in the plate.

Table I. Chemical Compositions of the Steels Investigated

	C	Mn	Si	S	P	Ti	Nb	B	Al	N
Nb steel	0.026	1.42	0.16	0.007	0.007	0.02	0.055	-	0.02	0.006
Nb + B steel	0.026	1.56	0.15	0.007	0.006	0.02	0.055	0.003	0.025	0.006

III. EXPERIMENTAL RESULTS

III-1. Stress relaxation after 25% prestrain

The stress relaxation data obtained after prestraining could be divided into three categories according to the way in which the stress decreased during holding. In the first type, the stress dropped at a steady rate after prestraining and then suddenly began to decrease more quickly until the load was almost completely relaxed. (This occurred after about 2 sec. in the Nb steel and 10 sec. in the Nb + B grade at 1000 °C (see Fig. 1a). It should be noted, however, that the relaxation rate during the rapid drop is slower in the Nb-B steel than in the B-free one. The break in the slope of the stress versus log time curve after which the stress decrease is faster is associated with the start of recrystallization. These results are in good agreement with those obtained earlier on the same steels using interrupted compression testing (5).

The second type of curve was obtained at an intermediate test temperature of 950 °C. In this case, the relaxation behaviour depends on the alloy type. In the Nb steel (see Fig. 1b), recrystallization is initiated after about 5 sec. and continues until 80 seconds; it is then arrested and a plateau in stress appears which lasts for about 350 sec. After a total elapsed time of about 430 sec., rapid relaxation is resumed again and the stress drops continously until the end of the test. This result indicates that there is an interaction between recrystallization and precipitation, and that the occurrence of precipitation leads to an interruption of the softening process in this case. In the Nb-B steel, only one stage of rapid softening is observed. Here, the only change in the relaxation behaviour is the appearance of a stress plateau indicating the beginning of precipitation after 37 sec. (Fig. 1b). It is of interest that the slopes of the relaxation lines on the present type of semi-log paper are approximately equal for the two steels in Figs. 1a and 1b (and in 1c below), as long as neither precipitation nor recrystallization is taking place.

The third type of stress relaxation curve is observed when the temperature is too low to permit recrystallization to take place prior to precipitation. This situation is illustrated in Fig. 1c for the two steels. Here it can be seen that the Nb-B steel has a higher yield strength than the B-free steel, although the relaxation slopes are similar. It is also evident that precipitation begins after about 7 and 18 sec. in the Nb-B and Nb steel, respectively. The sequences of metallurgical phenomena occurring in the two steels at the three temperatures are summarized in Table II.

From the tests carried out at 800 and 900 °C and by determining the relaxation arrest times as described above, precipitation-time-temperature (PTT) curves were established for the present materials (Fig. 2a). It is clear from these results that the presence of boron decreases the precipitation start time significantly from 35 sec. in the Nb steel to 10 sec. in the Nb-B steel at 900 °C. The difference in the finishing times increases to about 100 sec. The PTT curves have similar C shapes with noses around 800 to 850 °C. The occurrence of phase transformation prevented the attainment of lower test temperatures.

Table II. Hardening and Softening Processes Operating During Stress Relaxation.

	1000 °C	950 °C	850 °C
Nb + B Steel	Recovery Recrystallization	Recovery Precipitation Recrystallization	Recovery Precipitation Recrystallization
Nb Steel	Recovery Recrystallization	Recovery Recrystallization Precipitation Recrystallization	Recovery Precipitation Recrystallization

It is clear from the above results that the addition of boron to a Nb steel retards the recrystallization start time and accelerates the process of carbonitride precipitation. By contrast, the results obtained on two Nb-free reference steels (5,9) indicate that the addition of boron alone has almost no effect on the onset of recrystallization.

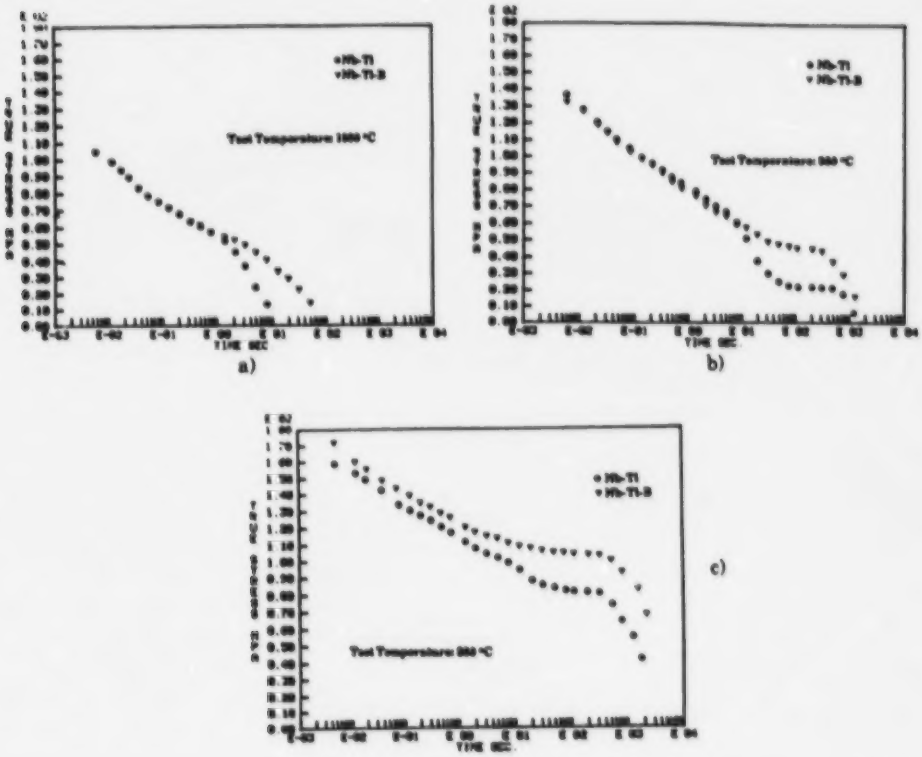

Fig.1. Comparison of stress relaxation data determined on the Nb and Nb-B steels after prestraining 25%.

III-2. Stress relaxation after 5% prestrain

In order to eliminate the interaction between recrystallization and precipitation, tests were carried out using a reduced prestrain of 5%, which is less than the critical strain for recrystallization. As in the previous case, the relaxation rates of the two steels were similar, although the Nb-B steel displayed higher levels of stress. The results obtained between 800 and 950 °C indicate that the precipitation process is faster in the Nb-B steel at all temperatures. The PTT curves obtained from the 5% prestrain relaxation data are shown in Fig. 2.b. Here again the PTT curves are of C shape and the influence of boron on the precipitation start time is clear. The addition affects both the time and temperature of the nose, which is at 830 °C and 10 sec. in the Nb-B steel and 800 °C and 20 sec. in the Nb steel. Thus it appears that the addition of boron accelerates strain-induced precipitation, even for prestrains as low as 5%.

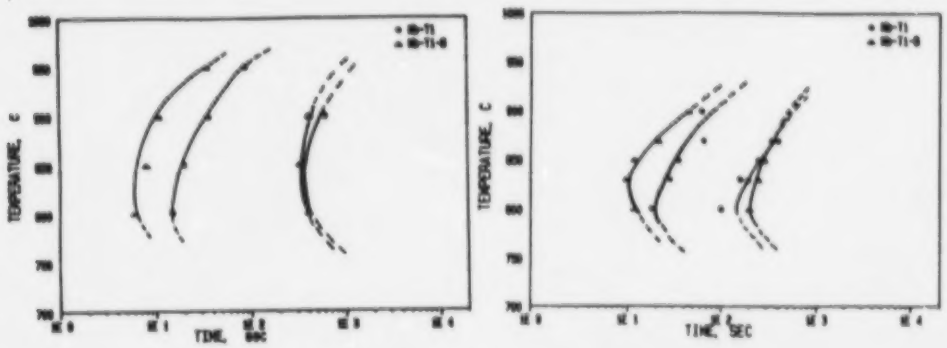

a) $\varepsilon = 25\%$ b) $\varepsilon = 5\%$

Fig.2. PTT curves for the two steels determined after two different prestrains.

III-3. Particle tracking autoradiography (PTA)

This technique is very useful for revealing the location of boron atoms and compounds in steel. It was employed on the Nb-B steel samples prestrained 5%, which were quenched at different stages of stress relaxation. The changes in the location of the boron at 850 °C as a function of time are illustrated in Fig.3. In the sample quenched after solutionizing at 1100 °C, a homogeneous distribution is observed (not presented in Fig. 3). Several seconds after deformation, the segregation of boron to the prior austenite grain boundaries is readily detectable, Fig. 3a, and several boron-containing precipitates can also be seen. These precipitates, which appear mainly at the grain boundaries, are probably ferroborocarbides (10) and are formed from the boron which segregates to the grain boundaries after deformation. As the holding time is increased to 200 and then to 900 sec., the grain boundary segregation gradually disappears and the number of boron containing precipitates increases (Figs. 3b and 3c). The diameters of these precipitates fall in the range 2 to 3 μm. In Fig. 3d, the microstructure of a part of Fig. 3c is shown at a higher magnification. Here, groups of etch pits are apparent within the grains, a geometry which was also observed in samples quenched after long holding times (1800 and 3600 sec.). This indicates that there are boron containing precipitates within the grains as well, in agreement with earlier workers (4). These are probably boron-containing, Ti-Nb carbonitrides, as will be discussed in more detail below.

From the PTA experiments, the following conclusions can be drawn : i) deformation induces boron grain boundary segregation; ii) this segregation is gradually transformed into grain boundary precipitation as the holding time is increased; iii) after long holding times, an agglomeration of etch pits within the grains is observed, which indicates the presence of small precipitates containing boron.

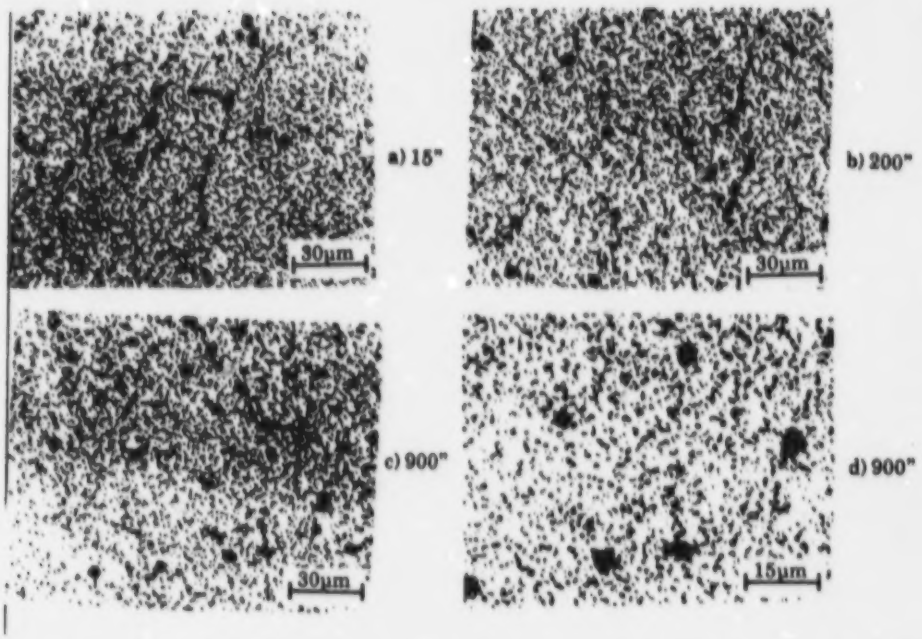

Fig.3. Distribution of boron in the Nb-B steel after a 5% prestrain at 850 °C and quenched after increasing holding times.

III-4. Electron microscopy

The technique of carbon extraction replication was employed to study the evolution in the distribution of the precipitates during stress relaxation testing. Electron micrographs of the Nb-B steel deformed 5% at 850 °C and quenched after 15, 900 and 3600 sec. are presented in Figs. 4 a,b and c, respectively. The equivalent micrographs for the Nb steel are illustrated in Figs. 5 a, b and c, respectively. In both steels, the precipitation is largely random, although in the Nb-B steel, several grain boundary precipitates are also observed, as already discussed above. The precipitate sizes were similar in the two steels, about 15 to 25 nm at the beginning of precipitation and more than 100 nm for the samples quenched after one hour. Energy dispersive X-ray analysis (EDX) was used to study the composition of the precipitates. The results show that there are four kinds of precipitates in the present materials : 1) undissolved TiN particles, which are formed at high temperatures; 2) (Ti,Nb) precipitates which are formed both in the matrix and at austenite grain boundaries; 3) a few matrix precipitates containing only Nb; and 4) ferroborocarbides at grain boundaries, which were only present in the Nb-B steel.

EDX analysis of the (Ti,Nb) matrix precipitates revealed that the Nb concentration of the precipitates increases with holding time. The two large grain boundary precipitates observed in Fig. 4c also contain large amounts of Nb. This result suggests that the small undissolved TiN particles can act as nucleation sites for Nb carbonitride precipitation.

Although a direct correlation between the precipitates observed in the optical micrographs (i.e. of the PTA samples)and in the electron micrographs (extraction replication samples) is not possible (because of the scale difference between the two methods), it appears that not all the grain boundary precipitates observed in the PTA studies are ferroborocarbides. Some of these particles contain B, Nb and Ti. The small matrix precipitates containing Nb or Ti and Nb probably contain B as well, and are therefore likely to be responsible for the agglomeration of etch pits observed in the PTA results.

Fig.4. Carbon extraction replicas showing the progress of precipitation in the Nb-B steel during stress relaxation at 850 °C.

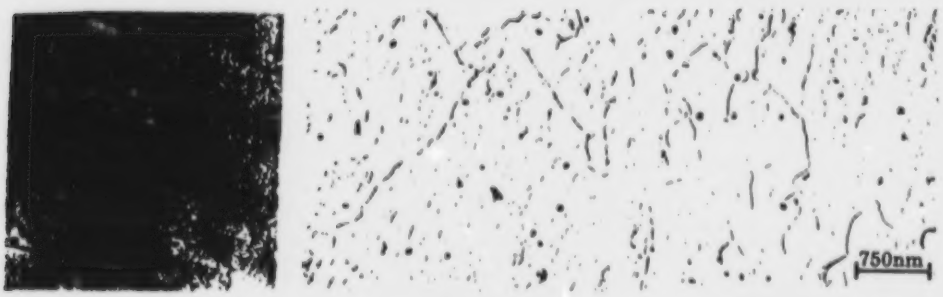

Fig.5. Carbon extraction replicas showing the progress of precipitation in the Nb steel during stress relaxation at 850 °C.

IV. DISCUSSION

IV-1. Effect of boron on the stress relaxation behaviour

A comparison of the results obtained on the B-free and B-modified steels indicates that the addition of boron influences both the recrystallization and precipitation processes. With respect to recrystallization, the stress relaxation tests carried out at 1000 and 950 °C show that the simultaneous presence of Nb and B retards recrystallization more effectively than that of Nb alone.

Similar results were obtained by Mavropoulos et al. (11), who used interrupted compression testing to measure fractional softening. Their observations covered the temperature range 900 to 1100 °C. With respect to the upper half of this range (i.e. 1000 to 1100 °C), no evidence for precipitation was observed, and they interpreted their measurements in terms of the solute drag theory. In the Nb steel, the segregation of Nb to the boundaries led to a drag force which depended on the ratio D_M/D_{GB}, where D_M and D_{GB} are the matrix and grain boundary diffusivities (5). When boron is added to the Nb steel, it increases D_M by forming Nb-B complexes and decreases D_{GB} by segregating at the grain boundaries (6). The addition of these two effects leads to an increase in the drag force.

At temperatures below 1000 °C, the retarding influence of boron can be interpreted as follows: i) Nb and B both segregate to the grain boundaries and retard the recrystallization start time; ii) the addition of boron accelerates the precipitation of the Nb carbonitrides, as shown in Figs. 2 and 3. The strain-induced precipitation of fine borocarbides prevents or arrests recrystallization (see Figs. 1b and 1c). Although the exact role of boron in the precipitation process is not yet clear, its presence could have two effects :

1) It increases the concentration of the interstitial elements from 0.12 atomic percent in the B-free steel to 0.14 atomic percent in the Nb-B grade (The presence of nitrogen is neglected here, as most of it is expected to have combined with Ti during solidification and subsequent cooling). This increases the concentration product of the precipitating species by about 14%, thus raising the driving force for precipitation. Such a driving force increase can in turn be responsible for the leftward movement of the C-curves in Figs. 2 a and b.

2) After deformation, because of the migration of Nb and B to the grain boundaries, sub-boundaries and dislocations, their concentration increases at these places, accelerating the precipitation of carbonitrides containing boron. The simultaneous presence of Nb and Ti in the precipitates seems to be due to the role played by small undissolved TiN precipitates as nucleation sites for Nb(C,B,N) or Nb(C,N) precipitation.

CONCLUSIONS

From the above experimental results, the following conclusions can be drawn:

1. The addition of boron to a Nb steel accelerates the strain-induced precipitation of (Ti,Nb)(C,B,N) and retards the onset of recrystallization in this way.

2. The use of particle tracking autoradiography shows that there is a clear evolution from the segregation of boron to dislocations and grain boundaries to precipitation at these sites. The acceleration of precipitation associated with boron addition can be attributed in turn to the increase in the concentration product of the precipitating species, and therefore in the driving force for precipitation.

REFERENCES

1) M.K. Koul and C.L. McVicker: Metal Progress, 11(1976), 2.

2) H. Tamehiro, M. Murata, R. Habu and M. Nagumo: Trans. ISIJ, 27(1987), 120.

3) H. Tamehiro, M. Murata, R. Habu and M. Nagumo: Trans. ISIJ, 27(1987), 130.

4) B.J. Thomas and G. Henry: Proc. Int. Conf. Boron Steels, The Metallurgical Society of AIME, Milwaukee, Wisconsin, 1979, 165.

5) L.T. Mavropoulos and J.J. Jonas : submitted to the Canadian Metallurgical Quart.

6) X.L.He, L.T.Mavropoulos and J.J.Jonas: this conference.

7) W.J. Liu and J.J. Jonas: Proc. Int. Conf. HSLA Steels '85, ASM International, Beijing, China, 1985, 253.

8) X.L.He and Y.Y.Chu: J.Phys.D: Appl.Phys., 16(1983), 1145.

9) M.Djahazi: Ph.D.Thesis, McGill University, Montreal, Canada, 1988.

10) Ph. Maitrepierre, J. Rofes-Vernis and D. Thivellier: Metall. Trans.A, 6(1975), 287.

11) L.T. Mavropoulos, G. Ruddle and J.J. Jonas: Proc. Int. Conf. HSLA Steels '85, ASM International, Beijing, China, 1985, 229.

GRAIN BOUNDARY SEGREGATION OF BORON DURING CONTINUOUS COOLING

X. L. He*†, Y. Y. Chu+ and J .J . Jonas*

*McGill University, Montreal, Canada

+ Beijing University of Iron and Steel Technology, China.

ABSTRACT

By means of particle tracking autoradiography (PTA), the segregation of boron along grain boundaries during continuous cooling was investigated in carbon-boron bearing steels and Fe-30%Ni alloys. The influence of deformation was also studied using hot compression testing. Such segregation involves the overlapping of two processes: (i) the equilibrium type, which takes place during isothermal holding and is not sensitive to cooling rate; (ii) the non-equilibrium type, which operates during cooling or deformation. Its intensity *increases* with quench temperature and a boron depleted zone forms next to the segregated region, whose width is sensitive to cooling rate. At lower temperatures, the segregation stems mainly from equilibrium considerations, whereas the non-equilibrium process is dominant in samples cooled from elevated temperatures. The transition temperature lies in the range 650-750°C and is associated with a segregation minimum. The width X of the boron-depleted zone can be used as a parameter to describe non-equilibrium segregation. The dependence of X on quench temperature T and cooling rate A is given by $X = H(T)/\sqrt{A}$. High temperature deformation before cooling increases the concentration of vacancy-boron complexes; it also intensifies the non-equilibrium segregation process, although it does not change the width of the boron-depleted zones.

---

† On leave from Beijing University of Iron and Steel Technology, China.

INTRODUCTION

Boron is one of the most potent elements for improving the hardenability of steels (1-4). The addition of boron (<40ppm by weight) also retards the recrystallization of HSLA steels after hot deformation, especially in Nb and Ti bearing grades (5-7). These phenomena have usually been attributed to the segregation of boron to austenite grain boundaries. There are currently two points of view about segregation to such interfaces. According to the first, the atom concentration at the boundary (C_e) is at the equilibrium level and is given approximately by

$$C_e = A\, C_0\, e^{Q/RT} \qquad (1)$$

where Q is the binding energy between the solute atom and the grain boundary, C_0 is the solute concentration in the matrix, and A is a constant related to the vibration entropy. According to this model, when the temperature is increased, the grain boundary segregation decreases exponentially. Conversely, when samples are cooled, the amount of grain boundary segregation increases and gradually reaches a new equilibrium level associated with the lower temperature (8-12). On the basis of equilibrium segregation, Seah (13) has successfully predicted the effects of time and temperature on the temper embrittlement of steel by phosphorus. Jandeska and Morral (14, 15) have also based their explanations of some aspects of boron segregation at grain boundaries on this model.

According to the second viewpoint, which is that of non-equilibrium as opposed to equilibrium segregation, the boron atoms are transported to the grain boundaries during cooling by a mechanism which involves the motion of excess vacancies towards the boundaries. In this case, the concentration of segregated

atoms at the interface is determined by the number of vacancy-solute complexes eliminated at the boundary during cooling. The latter quantity is sensitive to the temperature difference and cooling rate, but is not related to the level of equilibrium segregation at this temperature (16-22). The non-equilibrium segregation of boron to grain boundaries has been investigated by Williams et al. (23), He et al. (24-28), Faulkner (29) and Karlson and Norden (30). The problem has also been treated theoretically in Refs. (23, 25 and 28-30).

The aims of the present investigation were threefold: (i) to investigate the characteristics of boron segregation within a broad range of temperatures; (ii) to clarify the influence of quenching temperature, cooling rate and hot deformation on the two kinds of grain boundary segregation; and (iii) to describe the process of segregation during continuous cooling in a semi-quantitative manner. Such improvements in our understanding of the behaviour of boron in ferrous alloys can also help in the development of a suitable theory for the segregation of solute atoms to grain boundaries more generally.

2. EXPERIMENTAL MATERIALS AND METHODS

2.1. Experimental materials

Two types of materials were used in this investigation. The first (labelled C) consisted of carbon-boron bearing steels with different concentrations of carbon. Most of the steels were melted in an induction furnace and some were arc melted. After deoxidation and Ti addition, the boron was added in the furnace in each case. The ingots were heated to 1200°C and rolled into 30mm diameter bars or 13mm plates. The second series consisted of Fe-30%Ni alloys (labelled N); they were produced in a 25 Kg induction furnace and also contained a Ti addition for the

protection of the boron. These ingots were heated to 1150-1200°C and forged into blanks; they were then subjected to homogenization at 1200°C for 15 hours, reheated and forged again into 12 mm diameter bars. Specimens were machined from the bars or plates after the decarburized layers had been machined away. These layers were also assumed to have been depleted in boron. The chemical analyses of the alloys are shown in Table 1.

2.2. Heat treatment of the specimens

Treatment A: Cylindrical samples, 10 mm in diameter and 20 mm long, were heated to 1150°C or 1200°C for 30 min. under an argon atmosphere, furnace cooled to different temperatures and held isothermally for 30 min. and then either quenched in water or oil or air cooled. These treatments are described schematically in Fig.1a.

Treatment B: Disc specimens of the Fe-30%Ni alloys, 10 mm in diameter and 4mm thick, were heated to 1200°C for 30 min. under argon and furnace cooled to room temperature (no phase transformation takes place in this alloy). The cooling rate was less than 0.4°C/sec. when the temperature was above 1000°C, and less than 0.2°C/sec. when the temperature fell in the range 1000-650°C. After this pre-treatment, coarse particles of the boron constituent ($M_{23}(C,B)_6$) formed along the grain boundaries; these could readily be distinguished from the grain boundary segregation formed during subsequent heat treatment. The same coarse austenite grain size (about 120 μm) was observed in all the samples. The specimens were reheated to different temperatures for 30 min. and quenched in an ice-brine mixture or oil or cooled in air. The heat treatment schedule pertaining to these samples is shown schematically in Fig.1b.

Treatment C: Disc specimens, 10 mm in diameter and 4 mm thick, were cut from the 13mm carbon-boron steel plates, heated to 1100°C for 10 min. under argon, and then furnace cooled to 1000°C at a cooling rate of 0.15°C/sec. After isothermal holding for 5 min., the samples were hot compressed at a strain rate of 1 s^{-1} to a true strain of 0.25 using a 10,000 kg Instron testing machine. After various holding times, and either before or after deformation, the samples were quenched at different cooling rates (in ice-brine, water or oil). These samples were prepared so that the influence of deformation on the process of non-equilibrium segregation during cooling could be clarified. The relevant schematic diagram is given in Fig.1c.

Treatment D: Standard Jominy specimens, 25mm in diameter and 100mm long, were machined from the 30 mm diameter carbon-boron steel bars. The samples were heated to 1150°C for 30 min., then furnace cooled to different temperatures and end-quenched to room temperature, as shown in Fig. 1d. The boron distribution associated with different cooling rates was determined at different distances along the Jominy sample. The quench temperatures used in the four kinds of heat treatment are summarized in Table 2.

2.3. Determination of the boron distribution

After heat treatment, the boron depleted layer was removed from the surface of the samples, and the boron distribution was revealed with the aid of the particle tracking autoradiography (PTA) technique, which is based on the $^{10}B(n, \alpha)Li^{7}$ fission reaction (31). In the case of the Jominy specimens, samples were cut out at increasing distances from the quenched end, and the cooling rates at the corresponding locations are shown in Table 3. A cellulose acetate film was used as a solid detector, and the film-coated samples were irradiated in a beam of thermal

neutrons in suitable reactors*; the integrated fluxes ranged from 0.1 to 1.4 x 10^{15} neutrons/cm^2. After etching in a strong alkaline solution and coating with chromium, the films were examined under an optical microscope. The boron sensitivity of the PTA technique used in this study is about 1 ppm, and the spatial resolution is about 2 μm (32).

In order to enable the characteristics of the boron distribution revealed by the PTA method to be assessed semi-quantitatively, the samples used for measurement purposes were irradiated with the same integrated flux, 1.4 x 10^{15} neutron/cm^2, and the solid detector was cut from a single piece of cellulose acetate film. When different films were used, the etching times were adjusted to give etch pits of the same size. Typical size measurement results for single etch pits (without overlapping) are shown in Table 4, from which it can be seen that the average area of an etch pit is in the range 1.4 to 2.0 μm^2.

3. EXPERIMENTAL RESULTS

3.1. Characteristics of grain boundary segregation after quenching from different temperatures

We first consider carbon-boron steel C1, cylindrical samples of which were heated to 1150°C, furnace cooled to different temperatures and quenched in water (treatment A). The boron distribution revealed by PTA after light irradiation (10^{14} neutron/cm^2) is shown in Fig. 2a. It can be seen that the grain boundary segregation of boron becomes more marked as the quenching temperature is increased. After

*The irradiations were performed at the Institute of Atomic Energy, Beijing, China and Atomic Energy of Canada Limited, Chalk River, Ontario.

quenching from 1150°C, the segregation is nearly continuous, as revealed by the closely spaced etch pits. In the sample quenched from 950°C, there is considerably less segregation, and along the grain boundaries, the etch pit bands are much less distinct. Finally, in the sample quenched from 850°C, the segregation bands are no longer visible, and massive borocarbide precipitates formed during furnace cooling before quenching are seen instead.

The boron distributions in the same samples after irradiation to a higher flux level, 4×10^{14} neutron/cm^2, are shown in Fig. 2b. It can be seen that the dependence of the degree of segregation on quench temperature has the same tendency as in Fig. 2a. Nevertheless, differences in the level of segregation cannot be distinguished as clearly, because the density of etch pits is much higher, leading to overlapping. At the higher level of irradiation, the boron depleted zone near the grain boundaries shows up more clearly. As the quench temperature is increased, the width of the boron depleted zone increases and the degree of segregation is also raised.

The boron distribution in Fe-Ni alloy N2 quenched over a range of temperatures is shown in Fig. 3. The samples were heated to 1200°C, furnace cooled to different temperatures (no transformation) and quenched in oil (treatment A). Once again it can be seen that, as the quench temperature is decreased, the degree of boundary segregation revealed by PTA is diminished accordingly. There is an obvious boron depleted zone near the boundaries, which becomes narrower as the quench temperature is lowered. This tendency is similar to that displayed by the carbon steel in Fig. 2. When the quench temperature is decreased to 750°C, the degree of boron segregation reaches a minimum, as illustrated in Fig. 3d. When the quench temperature is decreased further, the grain boundary segregation increases

again, as shown in Figs. 3e and 3f, but in this case there is no boron depleted zone near the boundaries, and massive precipitates are again observed, as in Fig. 2.

The characteristics of boron segregation in the specimens cooled in water and air are similar to those for the specimens cooled in oil. At quench temperatures higher than 750°C, an effect of quenching medium can be seen. As the cooling rate is decreased (water to oil to air), the boron depleted zone is observed to widen, and the boundary segregation can be seen to become intensified, developing into a state of discontinuous aggregation. Concurrently, the transition temperature at which the boundary segregation minimum appears decreases, i.e. from 750 to 750-700 and then 700-650°C, respectively.

The distribution of boron revealed by PTA for Fe-Ni alloy N1 after treatment B (double reheating followed by ice-brine quenching from different reheating temperatures) is depicted in Fig. 4. In this case, the boron distribution is close to the equilibrium state associated with the quench temperature because the cooling rate used was high. It is evident that, on quenching from 1200°C, the boron distribution (Fig. 4a) is almost homogeneous, and the massive boron constituent formed during slow cooling from the first heat treatment is completely dissolved. Only a small amount of boron segregation is revealed by the PTA method at the grain boundaries. In the sample reheated to 800°C and quenched, the coarse boron carbides formed during pre-treatment are again absent, and there is some segregation, but it is rather weak (Fig. 4b). In the sample quenched from 750°C, massive borocarbides can be seen, together with some boron segregation on limited parts of the boundaries, Fig. 4c. When the samples were quenched from 600 and 550°C, in addition to the borocarbides, a degree of boundary segregation developed, which increases with decreasing quench temperature, as illustrated in Figs. 4d and 4e. When these

results are compared with those obtained from larger samples subjected to treatment A (Fig. 3), it is apparent that the segregation tendencies are similar below 700°C, and that they are not sensitive to cooling rate. By contrast, when cooling from higher temperatures, the characteristics of boron segregation shown in Fig. 3 and associated with oil quenching are not present when ice-brine quenching is employed.

The PTA results pertaining to the same alloy after heat treatment B, but followed in this case by cooling in air, are displayed in Fig. 5. Here, the borocarbide size distribution is similar to that illustrated in Fig. 4 (ice-brine quenching), but the dependence of the nature of the segregation on quench temperature is clearly different. For the samples air cooled from above 750°C, there is clear boundary segregation, and the amount of segregation *increases* with quench temperature. For the samples air cooled from 600 and 550°C, the boron distribution is similar to that displayed in Figs. 3 and 4. It is also apparent that the behaviors of the disc specimens cooled in air is similar to that of the cylindrical samples quenched in oil.

The boron distributions revealed by PTA in the Fe-30%Ni samples quenched in ice-brine on the one hand and air cooled on the other (treatment B) were measured semi-quantitatively. Forty to sixty straight grain boundary segments were analyzed in each sample. A parameter S/S_0 was defined to describe the degree of the segregation, where S and S_0 are the area fractions covered by etch pits in a narrow band 2 μm wide along the grain boundary and in the grain interior, respectively (27). The dependence of S/S_0 on quench temperature for alloy N1 is shown in Fig.6 . It can be seen that the behaviour is affected by cooling rate, although for holding temperatures below 700°C, the two curves are similar. At temperatures above 700°C, the trends diverge; in the air cooled material, S/S_0 *increases* with quench temperature, and so a segregation minimum is evident, Fig. 6b.

3.2. Dependence of boundary segregation on quench temperature and cooling rate in the high temperature region

The results described above indicate that the boundary segregation observed at the lower quench temperatures forms during isothermal holding, and is not particularly sensitive to cooling rate, Fig. 6a. By contrast, at the higher temperatures, segregation does not develop during isothermal holding, but requires the application of cooling. In the latter case, the degree of boron segregation revealed by the PTA method is sensitive to the quench temperature and the cooling rate, and a boron-depleted zone appears near the boundaries.

The average density of etch pits was measured in the grain boundary region (including the segregation band and depleted zone on both sides) and in the matrix. A parameter K was defined to describe this type of segregation:

The values of K for carbon-boron steel C2 heated to 1150°C and quenched in water from different temperatures (treatment A) are shown in Table 5. These measurements were corrected so as to take the effect of overlapping into account (31). It can be seen that all the K values are close to one, indicating that the boron at the boundaries originates in the boron depleted zones, and that this type of segregation takes place entirely during cooling.

The width of the boron depleted zones can be used to further characterize the nature of non-equilibrium segregation. For this purpose, the dependence of boron concentration on distance from the boundary was measured with an image analyzer

on the PTA micrographs (at 1000×). Boundary segments 50 mm in length were employed and narrow bands 2 mm in width were examined, see Fig. 7a. The area fractions covered by etch pits in the band S_x and in the matrix S_0 were measured. According to the PTA method (27), the etch pit density $\rho = E \Phi C$, where Φ is the integrated flux of thermal neutrons and E is an experimental constant. In the present case, Φ and E are constant, as is the size of a single etch pit, so the area fraction S is proportional to the boron concentration C.

$$S_x/S_0 = C_x/C_0 \qquad (2)$$

where C_x and C_0 are the concentrations in the narrow band and in the matrix, respectively. The relative boron concentration C_x/C_0 is shown schematically as a function of distance from the grain boundary in Fig. 7b (25, 26), and experimental results for the carbon-boron steel after treatment A are presented in Fig. 8a. The effect of quench temperature on the width of the boron depleted zone X is indicated in Fig. 8b.

The boron distributions corresponding to different cooling rates and quench temperatures were also determined on the Jominy specimens after treatment D. The concentration profiles and boron depleted zone widths were measured over the temperature range 840 to 1150°C and at cooling rates of 19 to 65°C/s. The results for carbon-boron steel C1 are given in Fig. 9. It can be seen that the boron depleted zone width X is proportional to the inverse square root of the cooling rate A:

$$X = H(T)/\sqrt{A} \qquad (3)$$

Here H(T) is a function of quench temperature and reflects the rate of grain boundary segregation as well as the effects of composition and other structural factors. By replotting these data against the inverse absolute temperatures of quenching, the activation energy of the segregation process was determined to be 0.92 eV (25,28).

3.3. The grain boundary segregation of boron after high temperature deformation

The PTA results obtained on undeformed disc specimens of carbon-boron steel C3 quenched from 1000°C in ice-brine are exhibited in Fig. 10a. It can be seen that the boron distribution is nearly homogeneous, indicating that little boron segregation occurs at this temperature. When the samples are quenched in water or oil, Figs. 10b and 10c, respectively, some boron segregates to the grain boundaries during cooling, the quantity increasing with decreasing cooling rate. Concurrently, the boron depleted zones are also widened.

Some similar samples were heated to 1100°C, furnace cooled to 1000°C, held isothermally for 5 min., and then compressed at a strain rate of 1 s^{-1} to a strain of 0.25 (treatment C). After hot deformation, the samples were quenched in ice-brine in less than 3 sec. The boron distribution revealed by PTA is exhibited in Fig. 11a, from which it can be seen that some boron segregation has taken place on the sub-boundaries that have formed by dynamic recovery within the austenite grains.

The boron distributions pertaining to samples quenched in water or in oil immediately after deformation are displayed in Figs. 11b and 11c. It is apparent that the non-equilibrium segregation of boron has taken place at austenite grain boundaries as well. The degree of segregation is greater than in the samples quenched before deformation at the same cooling rate. The boron depleted zones at the grain boundaries are also more clearly delineated, although the widths of these zones do not appear to have changed appreciably.

4. DISCUSSION

4.1. The two types of boron boundary segregation

It was demonstrated above that when the cylindrical samples were heated to the austenitizing temperature and cooled in water (Fig. 2) or in oil (Fig. 3), the degree of grain boundary segregation *increased* with quench temperature, and the width of the boron depleted zone increased concurrently. When a quench temperature of 700°C was used, this type of segregation was much weaker and the width of the boron depleted zone could not be measured. When the quench temperature was decreased further, the extent of grain boundary segregation increased again, although no boron depleted zones were observed next to the segregation bands in these cases.

The results obtained from the disc samples, Figs. 4 to 6, indicate that the low temperature form of segregation develops during isothermal holding at the quench temperature. The severity of the segregation decreases with increasing temperature and becomes too mild for ready detection at temperatures above 750°C. It is not sensitive to the cooling rates used in this investigation and does not lead to the appearance of boron depleted zones next to the boundaries. The characteristics of this type of segregation are those expected of equilibrium segregation, as described for example by McLean (8). Because the degree of segregation decreases rapidly with temperature, equilibrium segregation is only of importance at relatively low temperatures; in the present instance, the upper limit of this temperature range is 700°C.

At temperatures above 700°C, another type of segregation, referred to here as non-equilibrium segregation, is of greater importance. It does not take place during isothermal holding, and was not observed in the samples rapidly quenched in ice-

brine mixtures. The present results indicate that non-equilibrium segregation is sensitive to the rate of cooling, and that it leads to the formation of a boron depleted zone adjacent to the segregated boundary. The degree of segregation and the width of the boron depleted zone both increase with quench temperature under these conditions.

The segregation revealed by PTA in the samples cooled at intermediate rates can be described as the sum of these two types of process, as illustrated in Fig.12. Here the dependence of the equilibrium and non-equilibrium mechanisms on quench temperature is depicted by curves A and B, respectively, and the overall level of boron segregation is represented by curve C. There is a minimum at the transition temperature, near 700°C in the present case, below which boron segregation is controlled by equilibrium, and above which it is controlled by non-equilibrium considerations.

4.2. The quench induced non-equilibrium segregation of boron

Considerable experimental and theoretical work has been carried out on the non-equilibrium segregation (and desegregation) of solute atoms as induced by vacancy currents in metals and alloys (16-30). The non-equilibrium segregation of boron to grain boundaries during quenching has been analyzed by Williams et al. (23) as well as by Faulkner (29) on the basis of a model originally proposed by Aust and Westbrook (33) in 1965. The former authors have suggested that "segregation will occur if the complexes move rapidly enough to keep the complex concentration (C) reasonably uniform, and if the isolated impurities move so slowly that the total impurity concentration ((I)+(C)) is not also evened out " (23). In keeping with this view, they assumed that the diffusivity of the boron-vacancy complexes is 250 times

higher at all temperatures than that of the boron atoms and also much higher than that of the vacancies on their own.

However, the results of the present investigation, as well as related studies (24-28), indicate that boron segregation during cooling is the result of complexes diffusing through the *boron depleted zones* adjacent to the two sides of the boundary and eliminated there. The boron distribution remains homogeneous (and unchanged) solely in regions far from the grain boundaries. Furthermore, the segregated boron is obtained entirely from the boron depleted zones, so that the degree of segregation is independent of the grain size as long as the grain diameter is more than double the width of the boron depleted zone (for the present carbon-boron steel, the zone widths fall in the range 5-30 μm under the conditions employed in this paper). Thus the boron depleted zone width seems to be a more useful criterion for describing the dependence of non-equilibrium segregation on quench temperature than the grain size. It also enables the activation energy of the segregation process to be calculated directly from the experimental widths and equation (3).

4.3. High temperature deformation and the non-equilibrium segregation of boron

The results described above have shown that deformation before quenching increases the quantity of boron segregated to the grain boundaries (Figs. 10c and 11c), and also leads to segregation at sub-boundaries. By contrast, deformation seems to have little influence on the widths of the boron depleted zones. In order to account for the effect of deformation, it is useful to consider the total boron concentration C_T as consisting of two components: i) the concentration of single

atoms C_B, and ii) the concentration of boron-vacancy complexes C_C. Deformation prior to quenching increases the concentration of vacancies in the matrix, and is therefore likely to increase the concentration of the complexes. This is represented in Fig. 13 by an increase in C_C from C_{C1} (Fig. 13a) to C_{C2} (Fig. 13b), and by the decrease in the concentration of single boron atoms from C_{B1} to C_{B2}.

During cooling, the boron complexes are annihilated at the boundaries, and deposit boron at this location, freeing the vacancies. This leads to an increase in the boron concentration in the vicinity of the boundary, as indicated by the C_{S1} and C_{S2} curves in Figs. 13a and 13b for the undeformed and deformed samples, respectively. The total boron distribution in the material is represented by curves D_1 and D_2, from which the widths of the boron depleted zones in the two materials can be seen. As deformation does not seem to change the activation energy or the diffusion constant for complex diffusion, the width of the boron depleted zone is not shown as changing in Fig. 13, although the model indicates that the degree of boron depletion is more severe after deformation.

On the basis of the model described above, the non-equilibrium segregation of boron can be expected to have the following characteristics.

(1) After cooling, the quantity of boron segregated at a given boundary will only be related to the number of vacancies annihilated at the boundary. After cooling from elevated temperatures, the degree of such segregation will be considerably greater than expected from the equilibrium segregation mechanism.

(2) As non-equilibrium segregation is a dynamic phenomenon, it will be dispersed and homogenized by reverse diffusion once the supply of excess vacancies is exhausted.

(3) The excess vacancies induced by deformation will be annihilated at grain boundaries during isothermal holding. Thus deformation prior to isothermal holding can be expected to induce grain boundary segregation effects analogous to those produced by cooling.

5. CONCLUSIONS

(1) There are two kinds of boron segregation at austenite grain boundaries. The equilibrium type forms during isothermal holding, and is particularly marked after quenching from temperatures below 700°C. Its severity decreases with holding temperature and is not sensitive to the cooling rates used in this investigation. The non-equilibrium type forms during cooling; its severity as revealed by PTA *increases* with quench temperature, in opposition to the trend displayed by the equilibrium form. Under non-equilibrium conditions, a boron depleted zone forms next to the segregated region; its width is sensitive to cooling rate.

(2) The grain boundary segregation taking place during heat treatment involves the overlapping of these two kinds of segregation process. At lower temperatures, the segregation stems mainly from equilibrium considerations, whereas the non-equilibrium process becomes dominant in samples quenched from higher temperatures. The transition temperature in the present types of steel lies in the range 650-750°C and is associated with a segregation minimum.

(3) The degree of non-equilibrium segregation depends on cooling rate and quench temperature. The width X of the boron depleted zone can be used as a parameter to describe this type of segregation. The dependence of X on quench temperature T and cooling rate A is given by $X = H(T)/\sqrt{A}$, where H(T) is a function of T, as well as of composition and structure. For the present carbon-boron steels, the activation energy associated with the non-equilibrium segregation process is about 0.92 eV.

(4) High temperature deformation before quenching increases the concentration of vacancies and seems to increase the concentration of vacancy-boron complexes. During cooling, the non-equilibrium segregation process is intensified by the deformation-induced increase in the complex density, but deformation does not appear to change the width of the boron depleted zone or the mechanism of the segregation process.

ACKNOWLEDGMENTS

X.L. He and Y.Y. Chu thank Professor T. Ko for his encouragement and support. Drs. L. Tang and T.D. Xu took part in some of this research as graduate students in the Beijing University of Iron and Steel Technology. The study was supported in part by the Ministry of Metallurgical Industries of China and in part by the Canadian Steel Industry Research Association and the Natural Sciences and Engineering Research Council of Canada. Some of the steels were prepared at the Physical Metallurgy Research Laboratories of CANMET, Department of Energy Mines and Resources, Canada. Finally, X.L. He is grateful to McGill University for providing a Visiting Professorship.

REFERENCES

1. G.F. Melloy, P.R. Slimmon and P.P. Podgursky, Metall. Trans., 4, 2279 (1973).
2. D.T. Llewellyn and W.T. Cook. Metals Technology, 1, 517 (1974).
3. B.M. Kapadia, Hardenability Concepts with Applications to Steel, Eds. D.V. Doane and J.S. Kirkaldy, Metall. Soc. AIME, 448 (1978).
4. Ph. Maitrepierre, J. Rofes Vernis and D. Thivellier, Boron in Steel, Proc. Int. Symp. on Boron Steel, Milwaukee, Wisconsin, Sept. 1979, Eds. S.K. Banerji and J.E. Morral. Metall. Soc. AIME, 1 (1980).
5. T. Mavropoulos, J.J. Jonas and G.E. Ruddle. Proc. Int. Conf. on HSLA Steels '85, 4-8, Nov. 1985, Beijing, China, HSLA Steels: Metallurgy and Applications. Edited by J.M. Gray et al. ASM, 229 (1986).
6. H. Tamehiro, M. Murata, R. Habu and M. Nagumo, Trans. ISIJ, 27, 120 (1987).
7. H. Tamehiro, M. Murata, R. Habu and M. Nagumo. Trans. ISIJ, 27, 130 (1987).
8. D. McLean, Grain Boundaries in Metals, Oxford (1957).
9. E.D. Hondros and M.P. Seah. Int. Metal. Rev. 222, 262 (1977).
10. M. Guttmann and D. McLean. Interfacial Segregation. Eds. W.C. Johnson and J.M. Blakely. ASM, 261 (1979).
11. M.P. Seah. J.Phys.F: Metal Phys. 10, 1043 (1980).
12. T. Ogura, Trans.of the Japan Institute of Metals. 22, 109 (1981).
13. M.P. Seah, Acta Metall. 25, 345 (1977).
14. W.F. Jandeska Jr. and J.E.Morral. Metall. Trans., 3 2933 (1972).
15 J.E. Morral and W.F. Jandeska Jr. Metall. Trans., 11A 1628 (1980).
16. K.T. Aust, R.E. Hanneman, P. Niessen and J.H. Westbrook. Acta Metall. 16, 291 (1968).

17. T.R. Anthony. Acta Metall. 17, 603 (1969).

18. R.E. Hanneman and T.R. Anthony. Acta Metall. 17, 1133 (1969).

19. H. Wiedersich and P.R. Okamoto, Interfacial Segregation, Eds. W.C. Johnson and J.M. Blakely, ASM, 405 (1979).

20. D.R. Harries and A.D. Marwick, Phil. Trans. R. Soc. Lond. A295. 197 (1980).

21. P. Doig and P.E.J. Flewitt. Acta Metall. 29 1831 (1981).

22. P .Doig and P.E.J. Flewitt. Metall., Trans. 19A 399 (1987).

23. T.H. Williams, A.M. Stoneham and D.R. Harries, Metal Sci. 10, 14 (1976).

24. X.L. He, Y.Y. Chu and Z.S.Yu, Acta Metallurgica Sinica. 13, 225 (1977).

25. X.L. He, Y.Y. Chu and T. Ko, Proc. China-USA Bilateral Metallurgical Conference,. Beijing, China, 15-18, Nov., 532 (1981).

26. X.L. He, Y.Y. Chu and T. Ko. Acta Metallurgica Sinica 18, 1 (1982).

27. Y.Y.Chu, X.L.He, L.Tang, T.D.Xu and T.Ko. Proc. Int Symp. on Grain Boundary Structure and Related Phenomena, Minakami Spa, Japan, 25-29 Nov. 1985.

28. X.L. He, Y.Y. Chu and T. Ko. Acta Metallurgica Sinica 18, 11 (1982).

29. R.G. Faulkner, J. Materials Science 16, 373 (1981).

30. L. Karlson and H. Norden, Stainless Steels '84, The Institute of Metals, London, 85 (1985).

31. J.S. Armijo and H.S. Rosenbaum. J Appl. Phys. 38, 2064 (1967).

32. X.L. He and Y.Y. Chu. J. Phys. D: Appl. Phys. 16, 1145 (1983).

33. K.T. Aust and J.H. Westbrook, Lattice Defects in Quenched Metals, Academic Press, London, 771 (1965).

Table 1 Chemical compositions of the alloys tested (wt %)

Alloy	C	B	Mn	Ti	S	P	Ni
C1	0.54	0.0027	0.75	0.035	0.020	0.015	-
C2	0.24	0.0027	1.33	0.093	0.022	0.007	-
C3	0.03	0.0033	1.55	0.020	0.006	0.007	-
N1	0.008	0.0016	0.042	0.030	0.005	0.009	29.7
N2	0.07	0.0014	-	0.016	0.010	0.029	29.8

Table 2 Quench temperatures used in the various heat treatments

Treatment	Quench Temperature
A	1200, 1150, 1100, 1050, 950, 850, 800, 750, 700, 650
B	1200, 800, 750, 600, 550
C	1000
D	1150, 1100

Table 3 Cooling rates in Jominy bars as a function of distance

Jominy distance (mm)	0.5	1	2	3	4.5	6	7.5	9	12
Cooling rate (°C/s)	>450	>450	230	105	55	42	30	25	16.5

Table 4 Average etch pit areas, Fe-30%Ni alloy, quenched from the temperatures indicated

Quench temperature (°C)	840	840	750	750	600	600	550
Cooling medium	ice-brine	air	ice-brine	air	ice-brine	air	ice-brine
Average area for single etch pit (μm^2)	1.69	1.65	1.41	1.59	1.40	1.98	1.67
Number of pits counted	581	558	745	1233	1382	447	698
mean square deviation (μm^2)	0.025	0.027	0.024	0.018	0.014	0.028	0.024

Table 5 Values of K measured on steel C2 quenched from different temperatures

Quench temperature (°C)	840	920	1000	1080	1150
K	0.95	0.98	0.97	0.98	0.89

FIGURE CAPTIONS

Fig.1. Schematic diagrams of the different heat treatments employed.

Fig.2. Boron segregation at grain boundaries in carbon-boron steel C2 as a function of quench temperature; after irradiation to an integrated flux of: (a) 1×10^{14} neutron/cm^2. (b) 4×10^{14} neutron/cm^2.

Fig.3. Boron distribution revealed by PTA in Fe-Ni alloy N2 after treatment A (oil quenched from the temperatures indicated).

Fig.4. Boron distribution revealed by PTA in Fe-Ni alloy N1 after treatment B (ice-brine quenched from the temperatures indicated).

Fig.5. Boron distribution revealed by PTA in Fe-Ni alloy N1 after treatment B (air cooled from the temperature indicated).

Fig.6. Relative boron segregation at grain boundary S/S_0 as a function of quench temperature in Fe-Ni alloy N1. (a) quenched in ice-brine, (b) cooled in air.

Fig.7. Schematic illustration of the counting procedure employed to determine the boron concentration profiles.

Fig.8. (a) Boron concentration profiles for carbon-boron steel C1 quenched at 50°C/s from different temperatures. (b) Frequency histograms for the depleted zone widths X and segregation widths 2δ. (i) 1150°C, (ii) 1100°C, (iii) 960°C.

Fig.9. Width of boron depleted zone X as a function of cooling rate A and quench temperature, carbon-boron steel C1.

Fig.10. Boron distribution revealed by PTA in steel C3 prior to high temperature deformation; quenched from 1000°C in (a) ice-brine, (b) water and (c) oil.

Fig.11. Boron distribution revealed by PTA in steel C3 after hot compression to $\varepsilon = 0.25$; quenched at 1000°C in (a) ice-brine, (b) water and (c) oil.

Fig.12. Schematic illustration of roles of equilibrium and non-equilibrium boron segregation.

Curve A: The dependence of equilibrium segregation on quench temperature.

Curve B: The dependence of non-equilibrium segregation on quench temperature.

Curve C: The overall level of segregation in the samples cooled at intermediate rates.

Fig.13. Influence of deformation on the segregation of boron and on the width of the boron depleted zone. (a) quenched before deformation, (b) quenched after deformation.

C_T: Total boron concentration in matrix.

C_S: Concentration of single boron atoms in matrix.

C_C: Concentration of boron in complexes in matrix.

Curve C_S: Boron distribution after quenching arising from the presence of complexes.

Curve D: Total boron distribution after quenching.

X: Width of boron depleted zone.

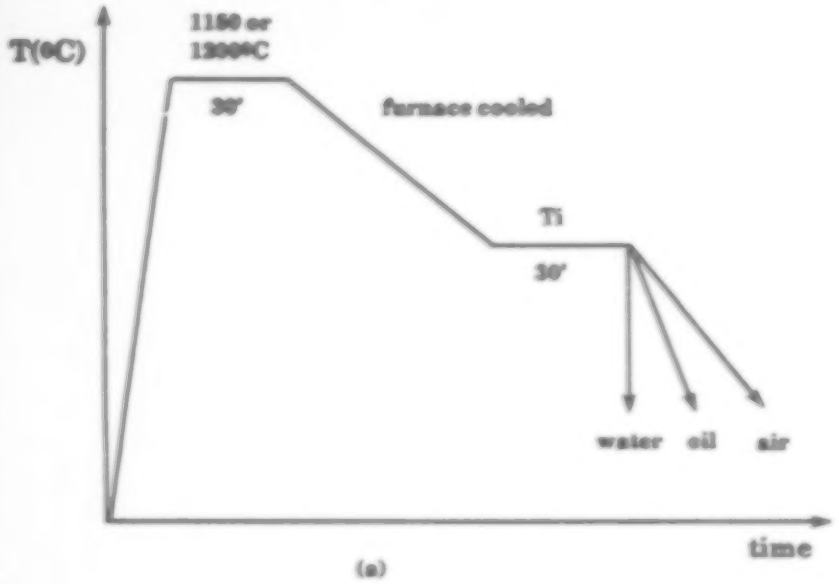
T(°C)
1150 or
1200°C
30'
furnace cooled
Ti
30'
water
oil
air
time

(a)

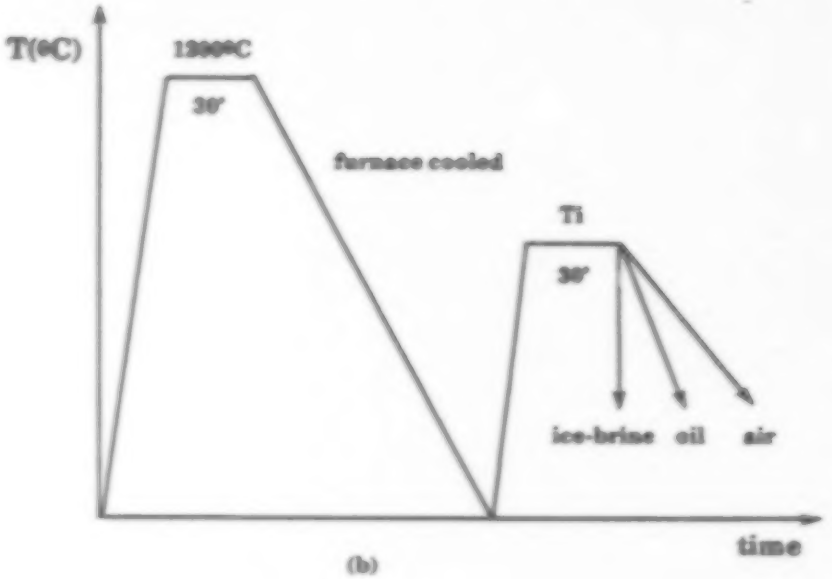
T(°C)
1200°C
30'
furnace cooled
Ti
30'
ice-brine
oil
air
time

(b)

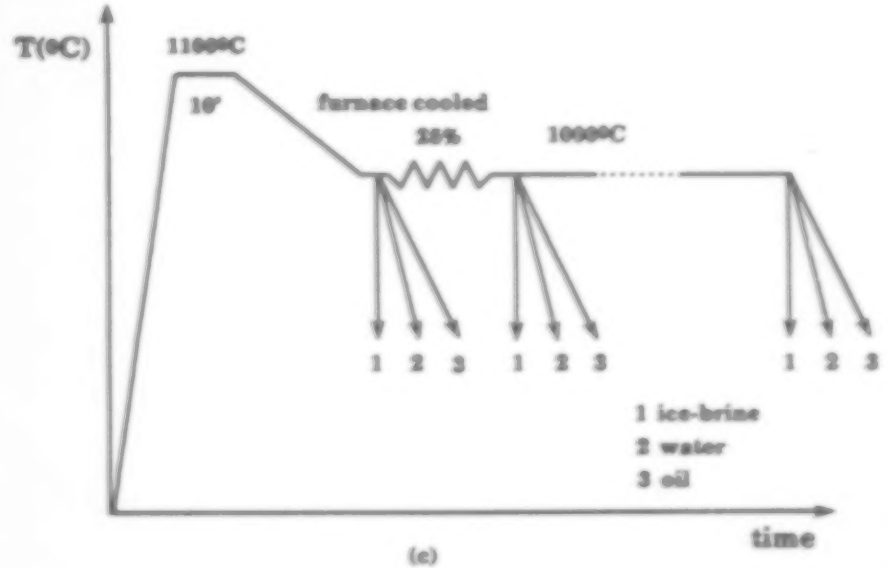
T(°C)
1100°C
10'
furnace cooled
25%
1000°C
1 2 3
1 2 3
1 2 3
1 ice-brine
2 water
3 oil
time

(c)

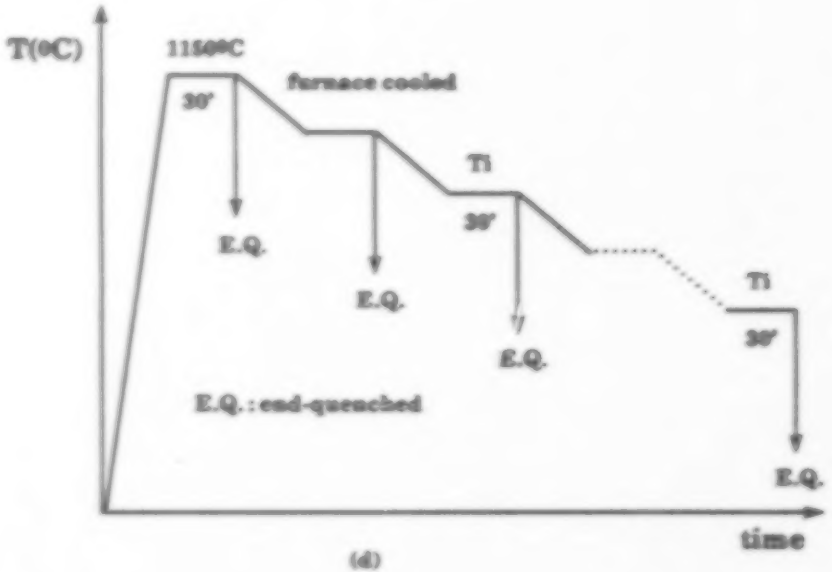
T(°C)
1150°C
30'
furnace cooled
Ti
30'
E.Q.
E.Q.
E.Q.
Ti
30'
E.Q.
E.Q. : end-quenched
time

(d)

Fig.1.

(a)

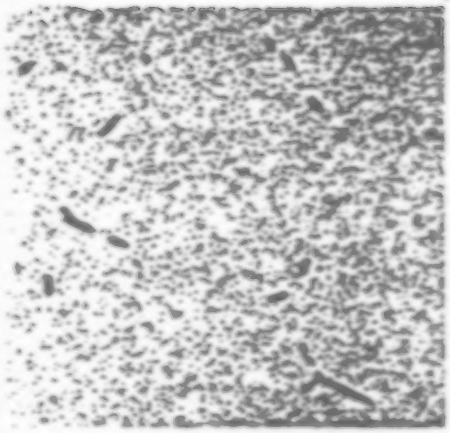

850°C

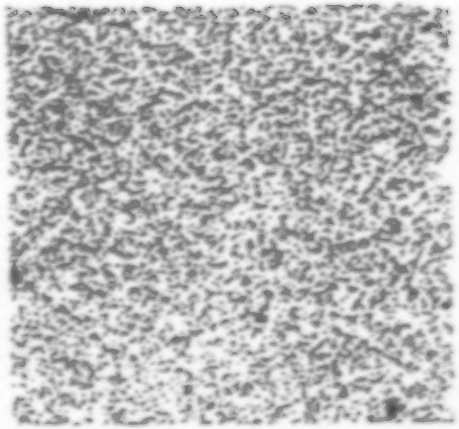

950°C

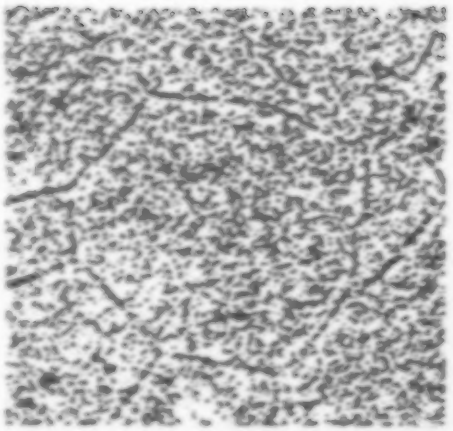

1100°C

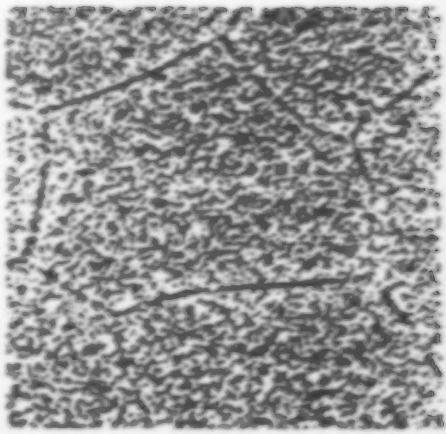

1150°C

(b)

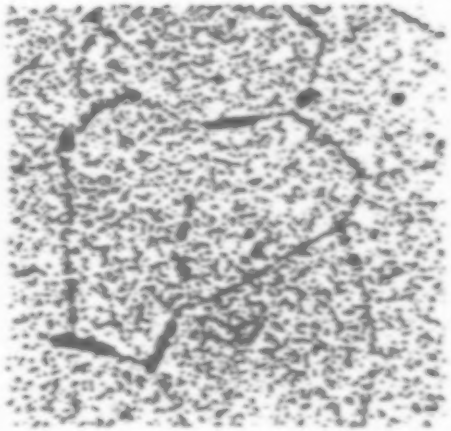

850°C

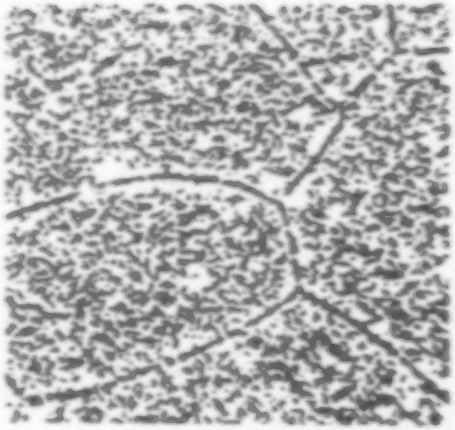

950°C

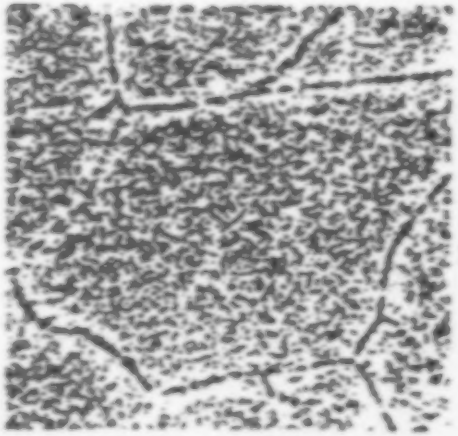

1100°C

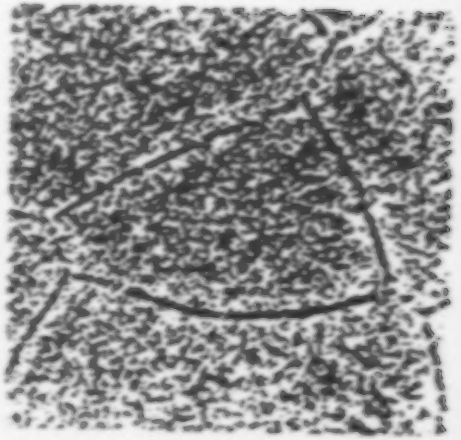

1150°C

Fig.2.

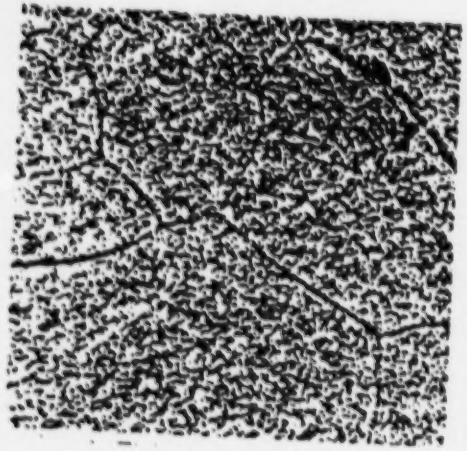

3(a) 1150°C

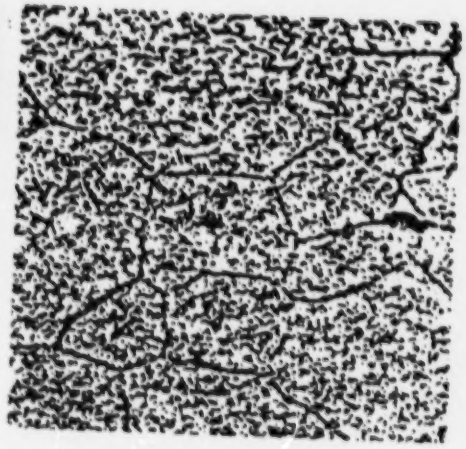

3(b) 1050°C

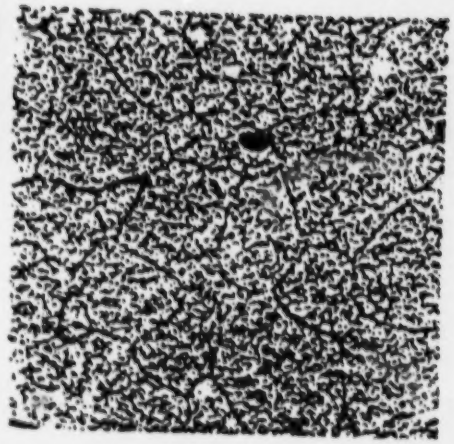

3(c) 950°C

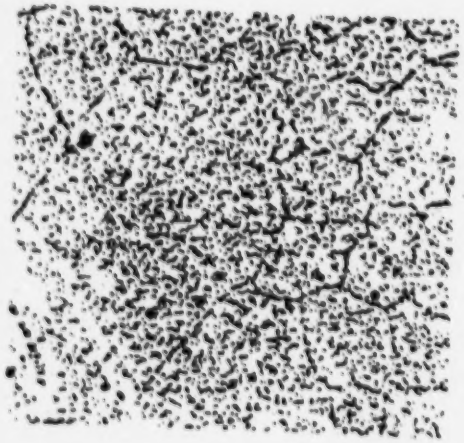

3(d) 750°C

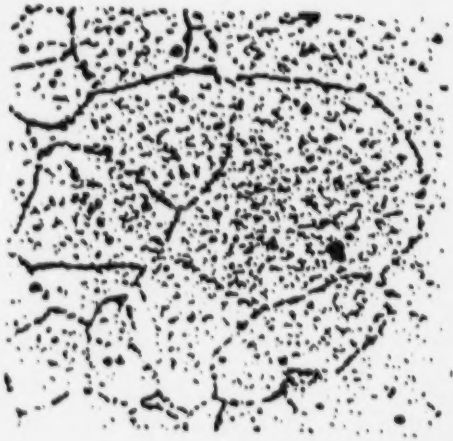

3(e) 700°C

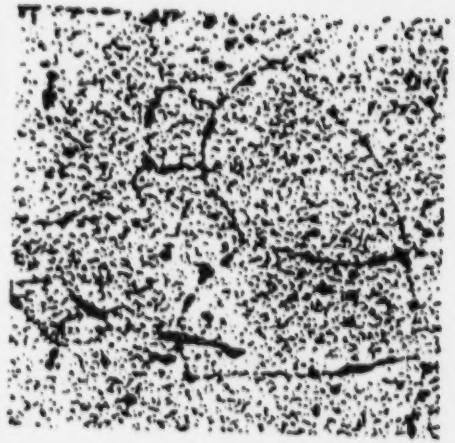

3(f) 650°C

Fig.3.

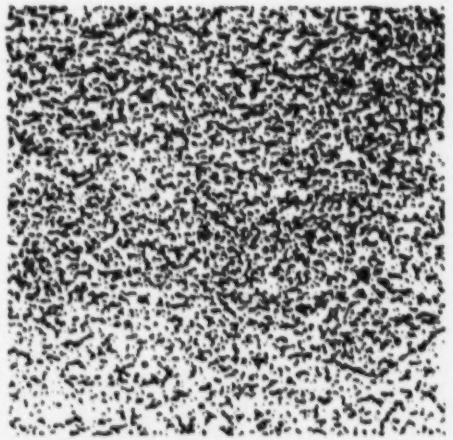

4(a) 1200°C

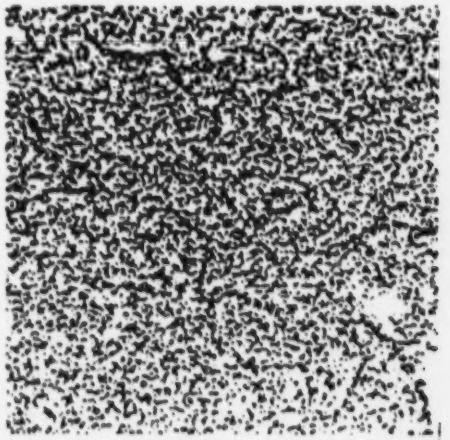

4(b) 800°C

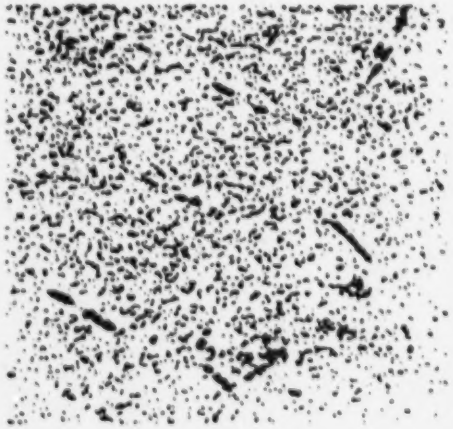

4(c) 750°C

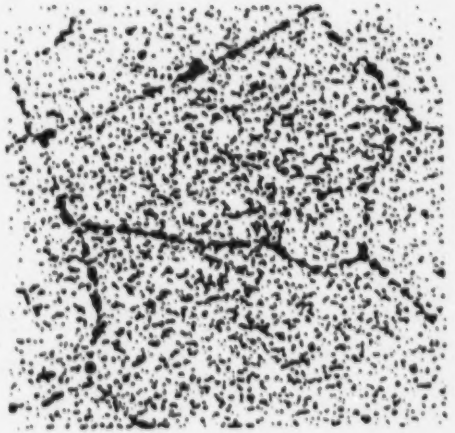

4(d) 600°C

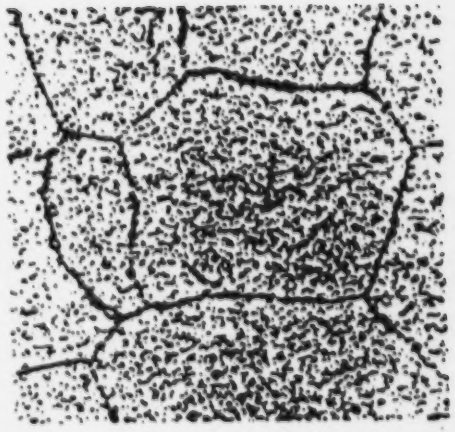

4(e) 550°C

Fig.4.

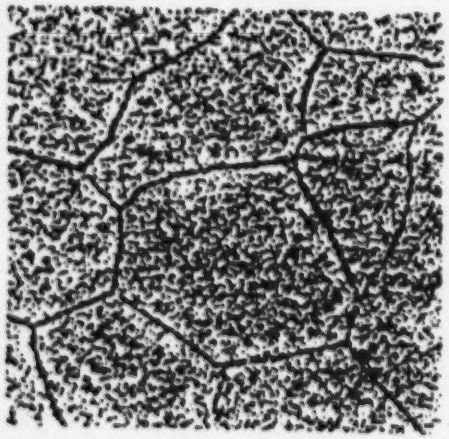

5(a) 800°C

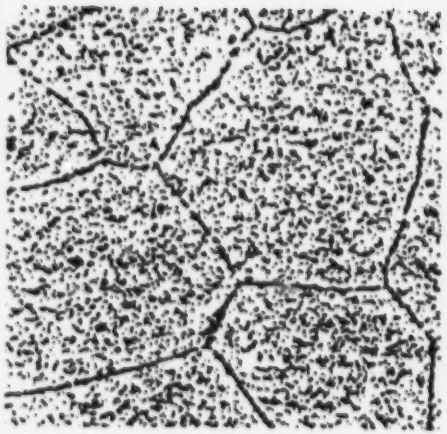

5(b) 750°C

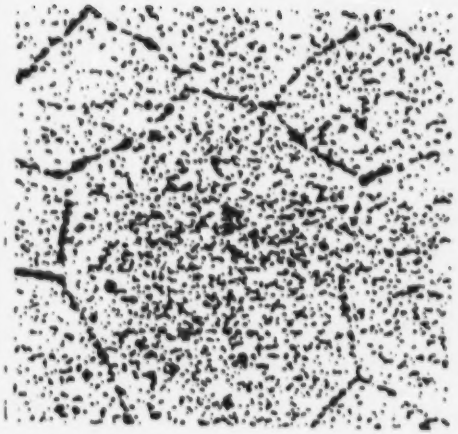

5(c) 600°C

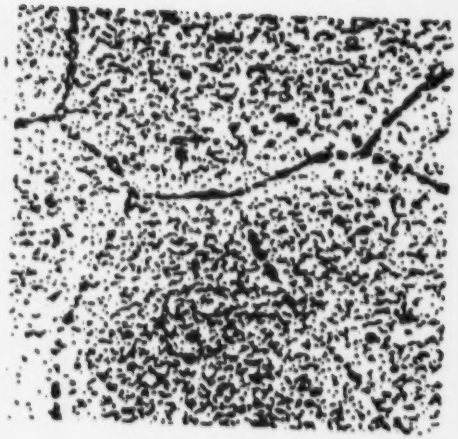

5(d) 550°C

Fig.5.

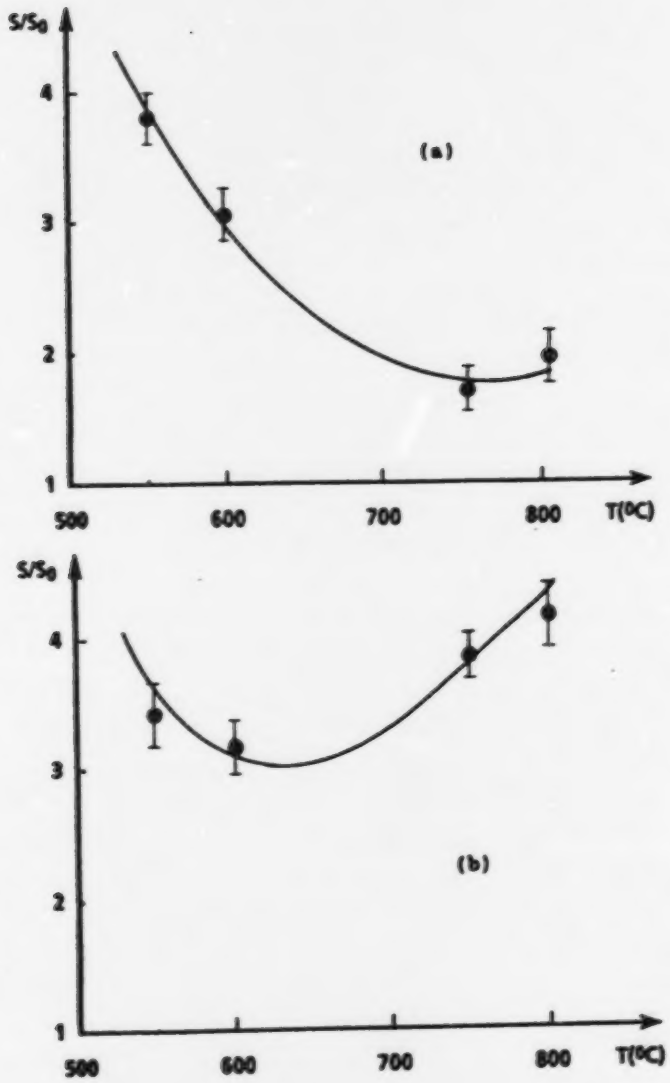

Fig.6.

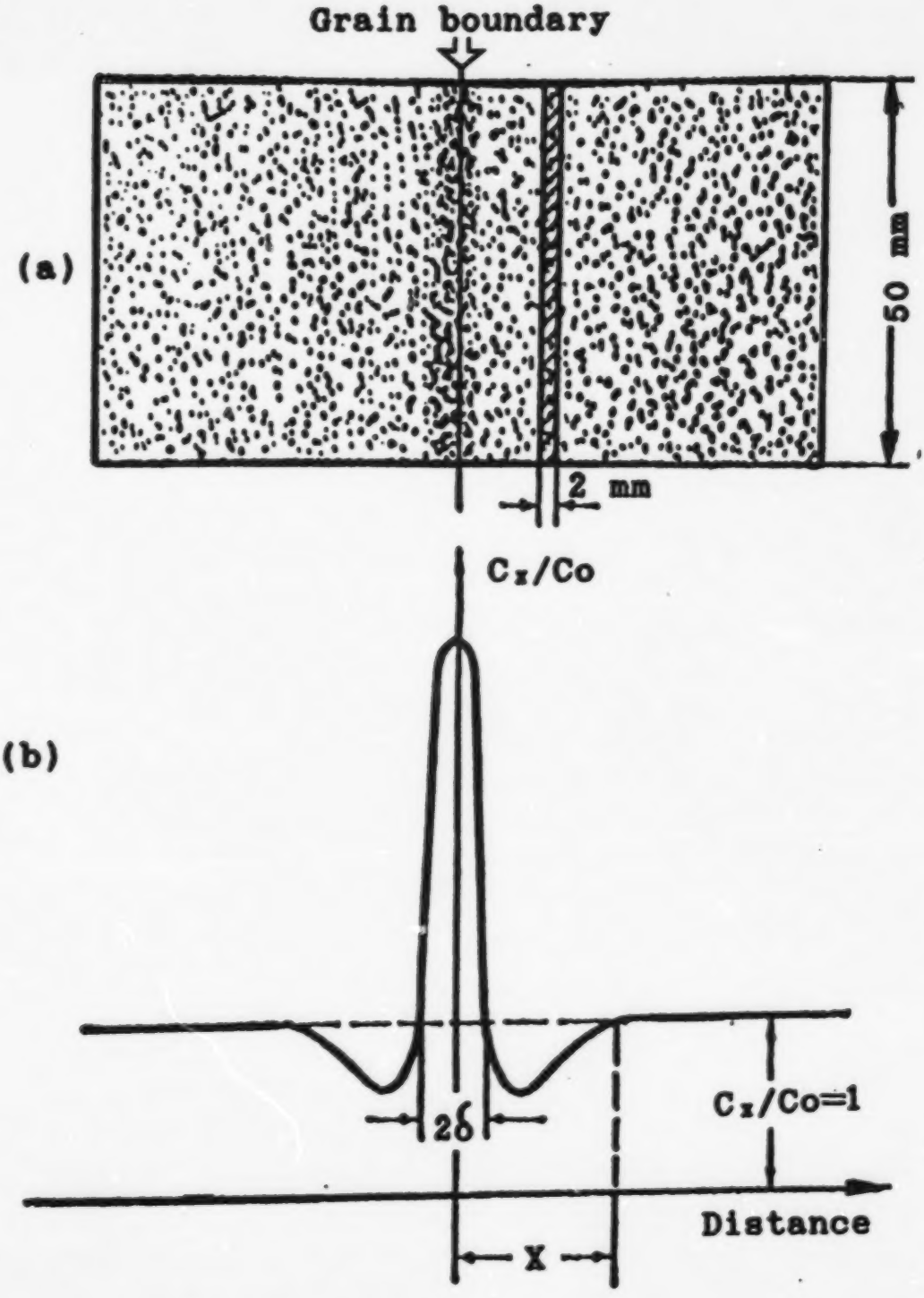

Fig.7.

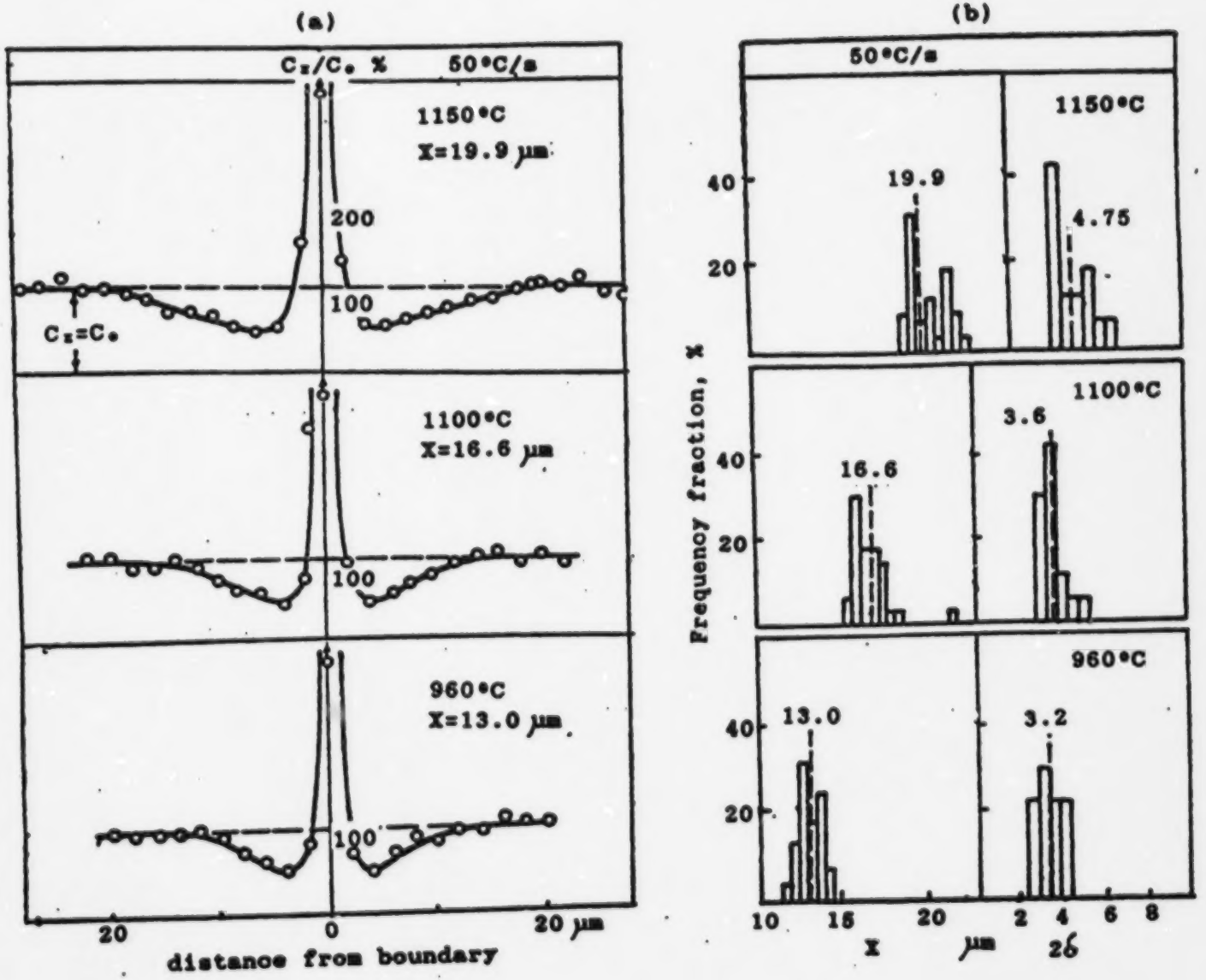
(a)
C_x/C_0 %
50°C/s
1150°C
X=19.9 μm
200
100
$C_x=C_0$
1100°C
X=16.6 μm
100
960°C
X=13.0 μm
100
20
0
20 μm
distance from boundary
(b)
50°C/s
1150°C
19.9
4.75
40
20
1100°C
16.6
3.6
40
20
960°C
13.0
3.2
40
20
Frequency fraction, %
10
15
20
2
4
6
8
X μm

Fig.8.

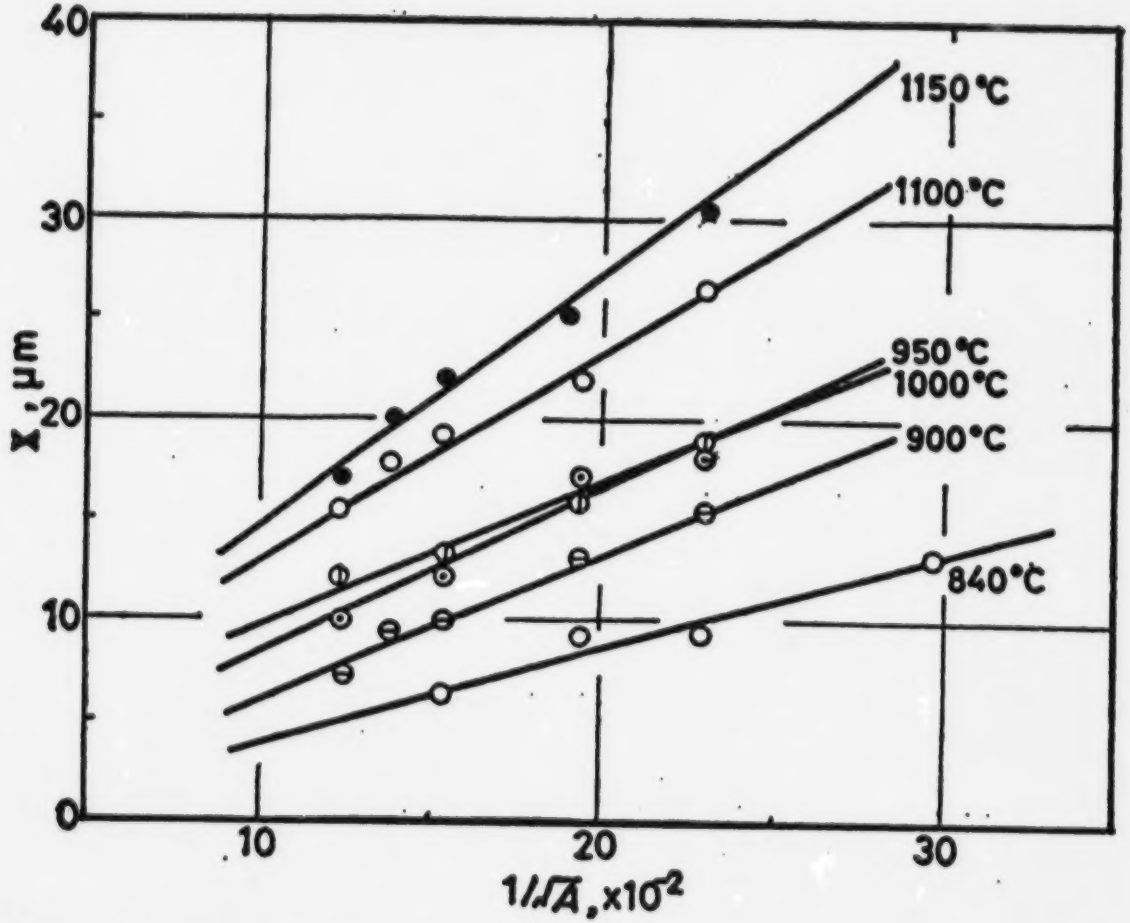
40
30
20
10
0
X, μm
1150°C
1100°C
950°C
1000°C
900°C
840°C
10
20
30
1/√A, x10⁻²

Fig.9.

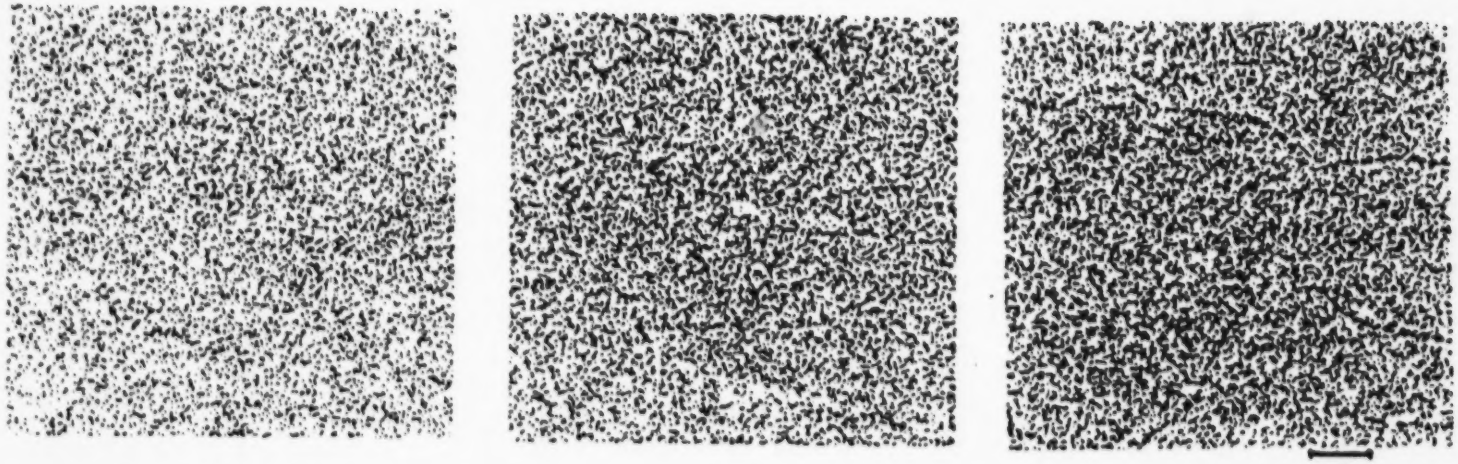

(a) in ice-brine (b) in water (c) in oil

Fig.10.

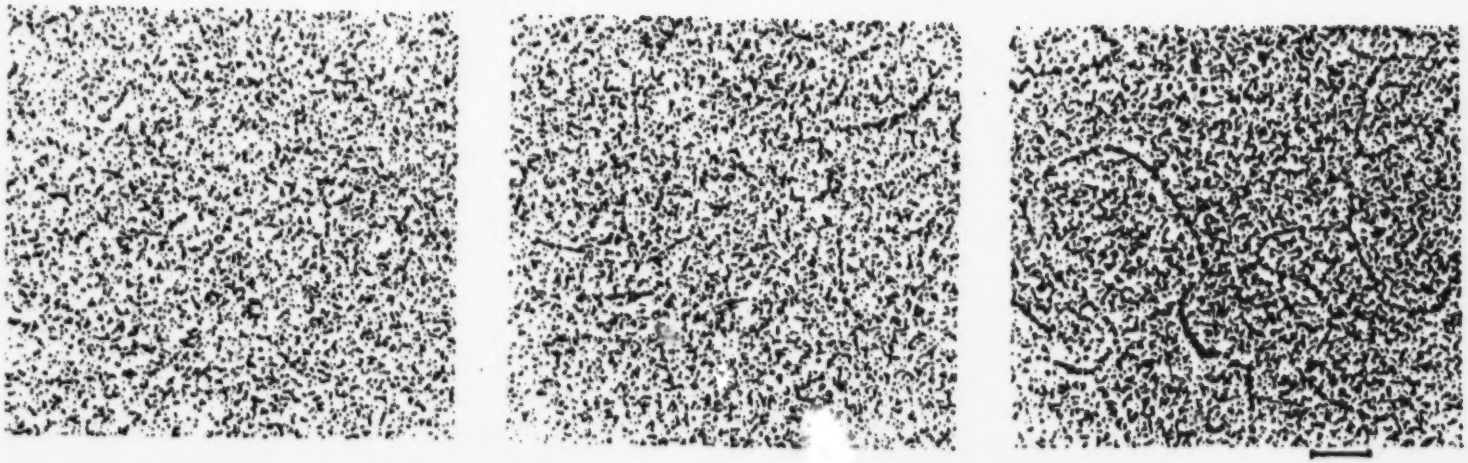

(a) in ice-brine (b) in water (c) in oil

Fig.11.

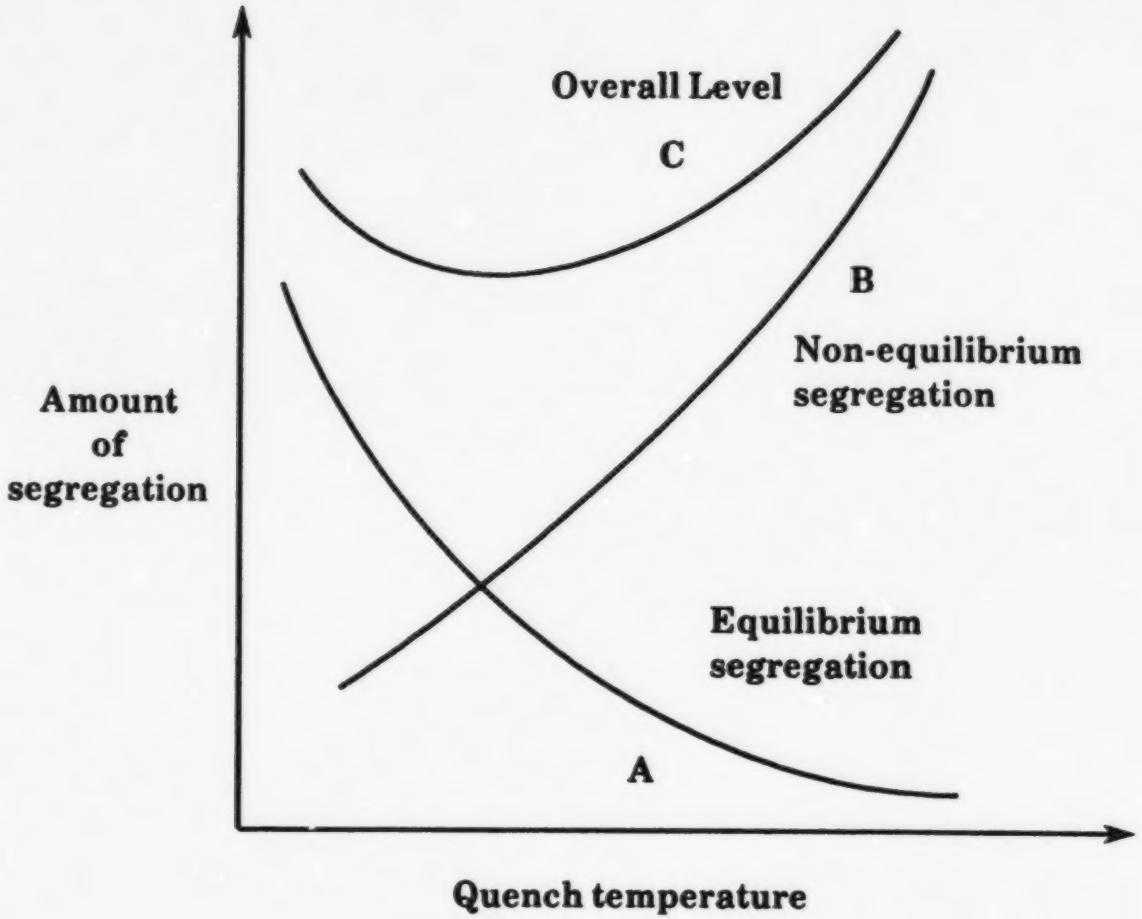
Overall Level
C
B
Non-equilibrium
segregation
Amount
of
segregation
Equilibrium
segregation
A
Quench temperature

Fig.12.

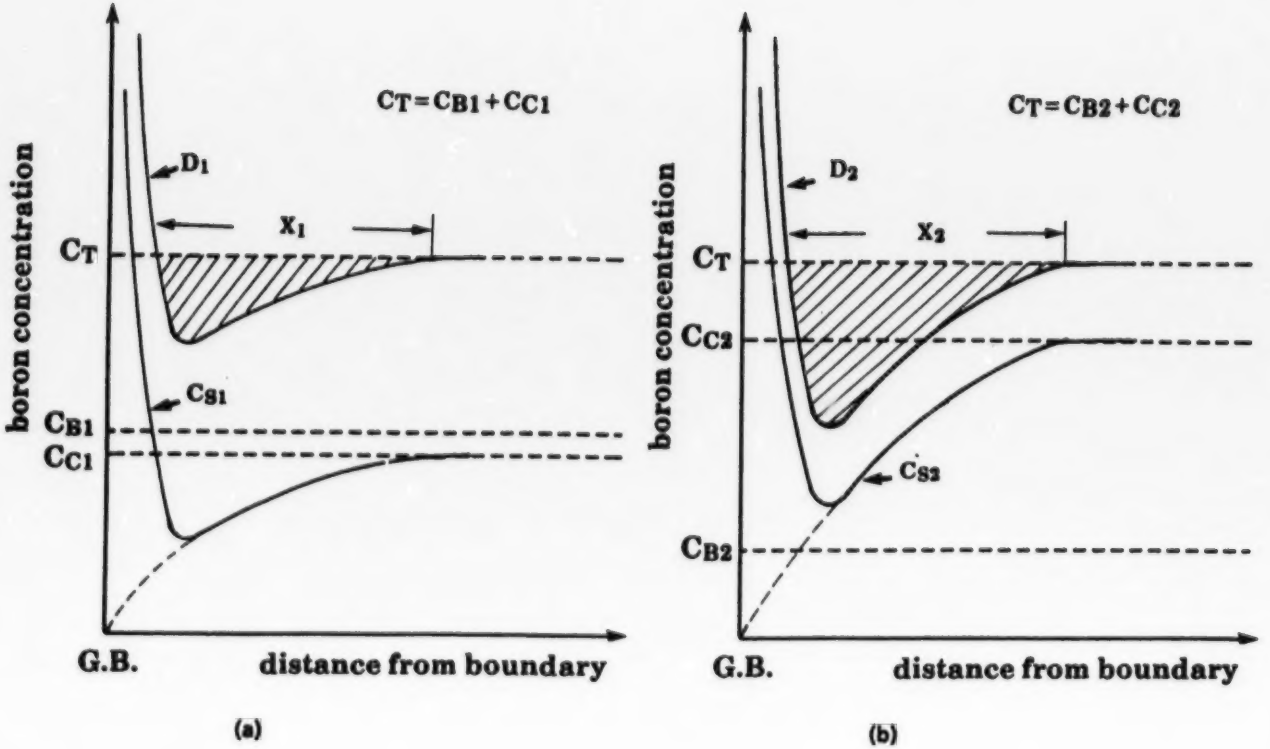
$C_T = C_{B1} + C_{C1}$
D_1
X_1
C_T
C_{S1}
C_{B1}
C_{C1}
boron concentration
G.B.
distance from boundary
(a)
$C_T = C_{B2} + C_{C2}$
D_2
X_2
C_T
C_{C2}
C_{S2}
C_{B2}
boron concentration
G.B.
distance from boundary
(b)

Fig.13.